

SUPPORTING INFORMATION

Synthesis of an extended halogen-bonded metal-organic structure in a one-pot mechanochemical reaction that combines covalent, coordination and supramolecular synthesis

Dominik Cinčić^{*a} and Tomislav Friščić^b

^a Department of Chemistry, Faculty of Science, University of Zagreb, Horvatovac 102a, HR-10000 Zagreb, Croatia

^b Department of Chemistry, McGill University and FRQNT Centre for Green Chemistry and Catalysis, 801 Sherbrooke St. W., Montreal, H3A 0B8 Canada

Email: dominik@chem.pmf.hr

Fax: +385 1 4606 341

Tel: +385 1 4606 362

Table of Contents

Experimental details	Materials, Solid-state synthesis, Solution synthesis, Thermal analysis, FTIR spectroscopy, Single-crystal X-ray diffraction experiments, Powder X-ray diffraction experiments	4
Table S1.	General and crystallographic data for Cu(naap) ₂ · tfib .	8
Figure S1.	Molecular structures of Cu(naap) ₂ · tfib showing the atom-labelling scheme. Displacement ellipsoids are drawn at the 30 % probability level and H atoms are shown as small spheres of arbitrary radius.	9
Figure S2.	PXRD pattern of pure napht reactant.	10
Figure S3.	PXRD pattern of pure aap reactant.	10
Figure S4.	PXRD pattern of pure copper acetate monohydrate.	11
Figure S5.	PXRD pattern of pure tfib reactant.	11
Figure S6.	PXRD patterns for mechanochemical and solution-based experiments involving napht and aap : a) napht , b) aap , c) compound Hnaap obtained by grinding in ball mill for 60 min in the presence of a small quantity of a mixture of EtOH and TEA [5% v/v of TEA], d) compound Hnaap obtained by solution-based method, e) calculated pattern for compound Hnaap .	12
Figure S7.	PXRD patterns for mechanochemical and solution-based experiments involving compound Hnaap and copper acetate monohydrate: a) compound Hnaap , b) copper acetate monohydrate, c) acetic acid solvate of Cu(naap) ₂ obtained by grinding in ball mill for 50 min in the presence of a small quantity of a mixture of EtOH and TEA [5% v/v of TEA], d) compound Cu(naap) ₂ obtained by solution-based method, e) acetic acid solvate of Cu(naap) ₂ after annealing at 200 °C for 30 min.	12
Figure S8.	PXRD patterns for mechanochemical and solution-based experiments involving compound Cu(naap) ₂ and tfib : a) compound Cu(naap) ₂ , b) tfib , c) compound Cu(naap) ₂ · tfib obtained by solution-based method, d) compound Cu(naap) ₂ · tfib obtained by grinding in ball mill for 50 min in the presence of a small quantity of nitromethane and e) calculated pattern for compound Cu(naap) ₂ · tfib .	13

Figure S9.	PXRD patterns for one-pot mechanochemical experiments: a) napht , b) aap , c) compound Hnaap , d) copper acetate monohydrate, e) tfib , f) compound $\text{Cu}(\text{naap})_2 \cdot \text{tfib}$ obtained by grinding of compound Hnaap , copper acetate monohydrate and tfib in ball mill for 50 min in the presence of a small quantity of nitromethane, g) compound $\text{Cu}(\text{naap})_2 \cdot \text{tfib}$ obtained by grinding of napht , aap , copper acetate monohydrate and tfib in ball mill for 60 min in the presence of a small quantity of nitromethane and h) calculated pattern for compound $\text{Cu}(\text{naap})_2 \cdot \text{tfib}$.	13
Figure S10.	IR spectrum for pure napht reactant.	14
Figure S11.	IR spectrum for pure aap reactant.	14
Figure S12.	IR spectrum for pure tfib reactant.	15
Figure S13.	IR spectrum for Hnaap prepared by solution-based method.	15
Figure S14.	IR spectrum for Hnaap prepared by LAG.	16
Figure S15.	IR spectrum for $\text{Cu}(\text{naap})_2$ prepared by solution-based method.	16
Figure S16.	IR spectrum for the product of grinding of copper acetate monohydrate and compound Hnaap , i.e. the acetic acid solvate of compound $\text{Cu}(\text{naap})_2$.	17
Figure S17.	IR spectrum for the product of grinding of copper acetate monohydrate and compound Hnaap after isothermal experiment at 200 °C.	17
Figure S18.	IR spectrum for $\text{Cu}(\text{naap})_2 \cdot \text{tfib}$ prepared by solution-based method.	18
Figure S19.	IR spectrum for $\text{Cu}(\text{naap})_2 \cdot \text{tfib}$ prepared by grinding of compound $\text{Cu}(\text{naap})_2$ and tfib .	18
Figure S20.	IR spectrum for $\text{Cu}(\text{naap})_2 \cdot \text{tfib}$ prepared by grinding of compound Hnaap and copper acetate monohydrate and tfib .	19
Figure S21.	IR spectrum for $\text{Cu}(\text{naap})_2 \cdot \text{tfib}$ prepared by grinding of napht , aap , copper acetate monohydrate and tfib .	19
Figure S22.	DSC curve for pure napht reactant.	20
Figure S23.	DSC curve for pure aap reactant.	20
Figure S24.	TG (black) and DTA (red) curve for pure copper acetate monohydrate.	21
Figure S25.	DSC curve for pure tfib reactant.	21
Figure S26.	DSC curve for Hnaap synthesised by solution-based method.	22
Figure S27.	DSC curve for Hnaap synthesised by grinding in ball mill for 60 min in the presence of a small quantity of a mixture of EtOH and TEA [5% v/v of TEA].	22
Figure S28.	TG (black) and DTA (red) curve for Hnaap synthesised by solution-based method.	23
Figure S29.	TG (black) and DTA (red) curve for $\text{Cu}(\text{naap})_2$ obtained by solution-based method.	23
Figure S30.	TG (black) and DTA (red) curve for the product (i.e. the acetic acid solvate of compound $\text{Cu}(\text{naap})_2$) obtained by grinding of copper acetate monohydrate and compound Hnaap in ball mill for 60 min in the presence of a small quantity of a mixture of EtOH and TEA [5% v/v of TEA].	24
Figure S31.	TG curve of isothermal experiment at 200 °C for the product of grinding of copper acetate monohydrate and compound Hnaap , i.e. the acetic acid solvate of compound $\text{Cu}(\text{naap})_2$.	24

Figure S32.	TG (black) and DTA (red) curve for Cu(naap) ₂ · tfib obtained by solution-based method.	25
Figure S33.	TG (black) and DTA (red) curve for Cu(naap) ₂ · tfib obtained by grinding of compound Cu(naap) ₂ and tfib in ball mill for 60 min in the presence of a small quantity of nitromethane.	25
Figure S34.	TG (black) and DTA (red) curve for Cu(naap) ₂ · tfib obtained by grinding of copper acetate monohydrate, compound Hnaap and tfib in ball mill for 60 min in the presence of a small quantity of a mixture of EtOH and TEA [5% v/v of TEA].	26
Figure S35.	TG (black) and DTA (red) curve for Cu(naap) ₂ · tfib obtained by grinding of copper acetate monohydrate, napht , aap and tfib in ball mill for 60 min in the presence of a small quantity of a mixture of EtOH and TEA [5% v/v of TEA].	26
Figure S36.	DSC curve for Cu(naap) ₂ · tfib obtained by grinding of copper acetate monohydrate, napht , aap and tfib in ball mill for 60 min in the presence of a small quantity of a mixture of EtOH and TEA [5% v/v of TEA].	27
Figure S37.	a) PXRD pattern of residue after TG experiment of compound Cu(naap) ₂ and b) calculated pattern for CuO.	28
Figure S38.	a) PXRD pattern of residue after TG experiment of compound Cu(naap) ₂ · tfib and b) calculated pattern for CuO.	28

EXPERIMENTAL DETAILS

MATERIALS

The starting materials, 2-hydroxy-1-naphthaldehyde (**napht**) and 4-aminoacetophenone (**aap**) were obtained from Acros Organics; copper acetate monohydrate was obtained from Kemika; and 1,4-tetrafluoroiodobenzene (**tfib**) was obtained from Merck. **Napht** was recrystallised from methanol and all other materials were used without further purification. Solvents were purchased from Kemika and T.T.T., Zagreb.

BALL MILLING EXPERIMENTS

Synthesis of **Hnaap**

For LAG experiment equimolar quantities of **napht** (0.129 g, 0.75 mmol) and **aap** (0.101 g, 0.75 mmol) were placed in a 10 mL stainless steel grinding jar along with 40 μ L of a mixture of EtOH and TEA [5% v/v of TEA] and two 7 mm-diameter stainless steel grinding balls. The mixture was then milled for 60 minutes in a Retsch MM200 Shaker Mill operating at 25 Hz frequency.

Synthesis of acetic acid solvate of **Cu(naap)₂**

For LAG experiment, compound **Hnaap** (0.174 g, 0.60 mmol) and copper acetate monohydrate (0.060 g, 0.30 mmol) were placed in a 10 mL stainless steel grinding jar along with 35 μ L of a mixture of EtOH and TEA [5% v/v of TEA] and two 7 mm-diameter stainless steel grinding balls. The mixture was then milled for 50 minutes in a Retsch MM200 Shaker Mill operating at 25 Hz frequency.

Synthesis of **Cu(naap)₂·tfib**

Single-step synthesis

For LAG experiment, compound **Cu(naap)₂** (0.030 g, 0.047 mmol) and **tfib** (0.019 g, 0.047 mmol) were placed in a 5 mL stainless steel grinding jar along with 15 μ L of nitromethane and two 4 mm-diameter stainless steel grinding balls. The mixture was then milled for 50 minutes in a Retsch MM200 Shaker Mill operating at 25 Hz frequency.

One-pot two-step synthesis

For LAG experiment, compound **Hnaap** (0.087 g, 0.30 mmol), copper acetate monohydrate (0.030 g, 0.15 mmol) and **tfib** (0.061 g, 0.15 mmol) were placed in a 10 mL stainless steel grinding jar along with 40 μ L of a mixture of EtOH and TEA [5% v/v of TEA] and two 7

mm-diameter stainless steel grinding balls. The mixture was then milled for 50 minutes in a Retsch MM200 Shaker Mill operating at 25 Hz frequency.

One-pot three-step synthesis

For LAG experiment, **napht** (0.052 g, 0.30 mmol), **aap** (0.041 g, 0.30 mmol), copper acetate monohydrate (0.030 g, 0.15 mmol) and **tfib** (0.061 g, 0.15 mmol) were placed in a 10 mL stainless steel grinding jar along with 40 μ L of a mixture of EtOH and TEA [5% v/v of TEA] and two 7 mm-diameter stainless steel grinding balls. The mixture was then milled for 60 minutes in a Retsch MM200 Shaker Mill operating at 25 Hz frequency.

SOLUTION SYNTHESIS

To monitor solid-state experiments, as well as to facilitate the characterisation of new materials by single-crystal X-ray diffraction, solid-state experiments were accompanied by conventional solution-based experiments. Crystal and molecular structures of **Hnaap** has been previously reported, CCDC code IXAPOM¹.

Synthesis of **Hnaap**

Equimolar quantities of **aap** (1.35 g, 0.01 mol) and **napht** (1.72 g, 0.01 mol), were dissolved in hot methanol (15 mL and 35 mL, respectively). The solutions were mixed and the resulting mixture left at room temperature. Orange precipitate appeared after a period of 1 day. It was separated from the mother liquor by filtration, and washed with methanol.

Synthesis of **Cu(naap)₂**

A clear solution of copper acetate monohydrate (0.199 g, 0.001 mol) in 50 mL methanol was added to a solution of compound **Hnaap** (0.579 g, 0.002 mol) in 70 mL acetonitrile. The resultant mixture was refluxed for 3 h and the brown precipitate was separated from mother liquor by filtration, and washed with methanol.

Synthesis of **Cu(naap)₂·tfib**

Equimolar quantities of compound **Cu(naap)₂** (0.64 g, 1.0 mmol) and **tfib** (0.40 g, 1.0 mmol), were dissolved in a hot mixture of ethanol and tetrahydrofuran (24 mL, 1:2). The resulting mixture left at room temperature. Brown crystals appeared after a period of 1 day. It was separated from the mother liquor by filtration, and washed with methanol.

THERMAL ANALYSIS

DSC measurements were performed on a Mettler-Toledo DSC823^e module in sealed aluminium pans (40 μ L), heated in flowing nitrogen (150 mL min⁻¹) at a rate of 10 °C min⁻¹. TG measurements were performed on a Mettler-Toledo TGA/SDTA 851^e module in sealed aluminium pans (40 μ L), heated in flowing oxygen (150 mL min⁻¹) at a rate of 10 °C min⁻¹. The data collection and analysis was performed using the program package STAR^e Software 9.01.²

FTIR SPECTROSCOPY

Infrared spectra were recorded on a PerkinElmer Spectrum Two FTIR spectrophotometer using a KBr pellet. The data collection and analysis was performed using the program package PerkinElmer Spectrum (version 10.4.2.279).

SINGLE-CRYSTAL X-RAY DIFFRACTION EXPERIMENTS

The crystal and molecular structures of Cu(**naap**)₂·**tfib** was determined by single crystal X-ray diffraction. Details of data collection and crystal structure refinement are listed in Table S1. The diffraction data were collected at 292 K for all compounds. Diffraction measurements were made on an Oxford Diffraction Xcalibur Kappa CCD X-ray diffractometer with graphite-monochromated MoK α ($\lambda = 0.71073 \text{ \AA}$) radiation. The data sets were collected using the ω scan mode over the 2θ range up to 54°. Programs CrysAlis CCD³ and CrysAlis RED³ were employed for data collection, cell refinement, and data reduction. The structures were solved by direct methods and refined using the SHELXS and SHELXL programs, respectively.⁴ The structural refinement was performed on F² using all data. The hydrogen atoms not involved in hydrogen bonding were placed in calculated positions and treated as riding on their parent atoms [C–H = 0.93 Å and $U_{\text{iso}}(\text{H}) = 1.2 U_{\text{eq}}(\text{C})$] while the others were located from the electron difference map. All calculations were performed using the WINGX crystallographic suite of programs.⁵ The molecular structures of compounds are presented by ORTEP-3⁶ and their molecular packing projections were prepared by Mercury.⁷

POWDER X-RAY DIFFRACTION EXPERIMENTS

PXRD experiments of the samples were performed on a PHILIPS PW 1840 X-ray diffractometer with CuK α 1 (1.54056 Å) radiation at 40 mA and 40 kV. The scattered intensities were measured with a scintillation counter. The angular range was from 3 to 50°

(2θ) with steps of 0.02° , and the measuring time was 0.5 to 1 s per step. The data collection and analysis was performed using the program package Philips X'Pert.⁸

References

1. S. Yüce, A. Özek, Ç. Albayrak, M. Odabasoglu and O. Büyükgüngör, *Acta Crystallogr.*, E60, **2004**, o1217.
2. STARe Software V.9.01., MettlerToledo GmbH, 2006.
3. Oxford Diffraction, Oxford Diffraction Ltd., Xcalibur CCD system, CrysAlis CCD and CrysAlis RED software, Version 1.170, 2003.
4. G. M. Sheldrick, *Acta Cryst. A* **2008**, 64, 112.
5. L. J. Farrugia, WinGX, *J. Appl. Cryst.* **1999**, 32, 837.
6. L. J. Farrugia, ORTEP-3 for Windows, *J. Appl. Cryst.* **1997**, 30, 565.
7. C. F. Macrae, I. J. Bruno, J. A. Chisholm, P. R. Edgington, P. McCabe, E. Pidcock, L. Rodriguez-Monge, R. Taylor, J. v. d. Streek and P. A. Wood, *J. Appl. Crystallogr.* **2008**, 41, 466.
8. Philips X'Pert Data Collector 1.3e, Philips Analytical B. V. Netherlands, 2001; Philips X'Pert Graphic & Identify 1.3e Philips Analytical B. V. Netherlands, 2001; Philips X'Pert Plus 1.0, Philips Analytical B. V. Netherlands, 1999.

Table S1. General and crystallographic data for Cu(**naap**)₂·**tfib**.

Compound Cu(naap) ₂ · tfib	
Molecular formula	(CuC ₃₈ H ₂₈ N ₂ O ₄)(C ₆ F ₄ I ₂)
M_r	1042.02
Crystal system	triclinic
Space group	$P \bar{1}$
Crystal data:	
$a / \text{\AA}$	8.093(5)
$b / \text{\AA}$	9.502(5)
$c / \text{\AA}$	12.751(5)
$\alpha / ^\circ$	82.472(5)
$\beta / ^\circ$	82.927(5)
$\gamma / ^\circ$	86.586(5)
$V / \text{\AA}^3$	963.8(9)
Z	1
$D_{\text{calc}} / \text{g cm}^{-3}$	1.795
$\lambda(\text{MoK}\alpha) / \text{\AA}$	0.71073
T / K	295
Crystal size / mm ³	0.13x0.22x0.51
μ / mm^{-1}	2.235
$F(000)$	509
Refl. collected/unique	11870 / 4192
Data/restraints/parameters	259
$\Delta\rho_{\text{max}}, \Delta\rho_{\text{min}} / \text{e \AA}^{-3}$	0.363; -0.584
$R[F^2 > 4\sigma(F^2)]$	0.0363
$wR(F^2)$	0.0879
Goodness-of-fit, S	0.984

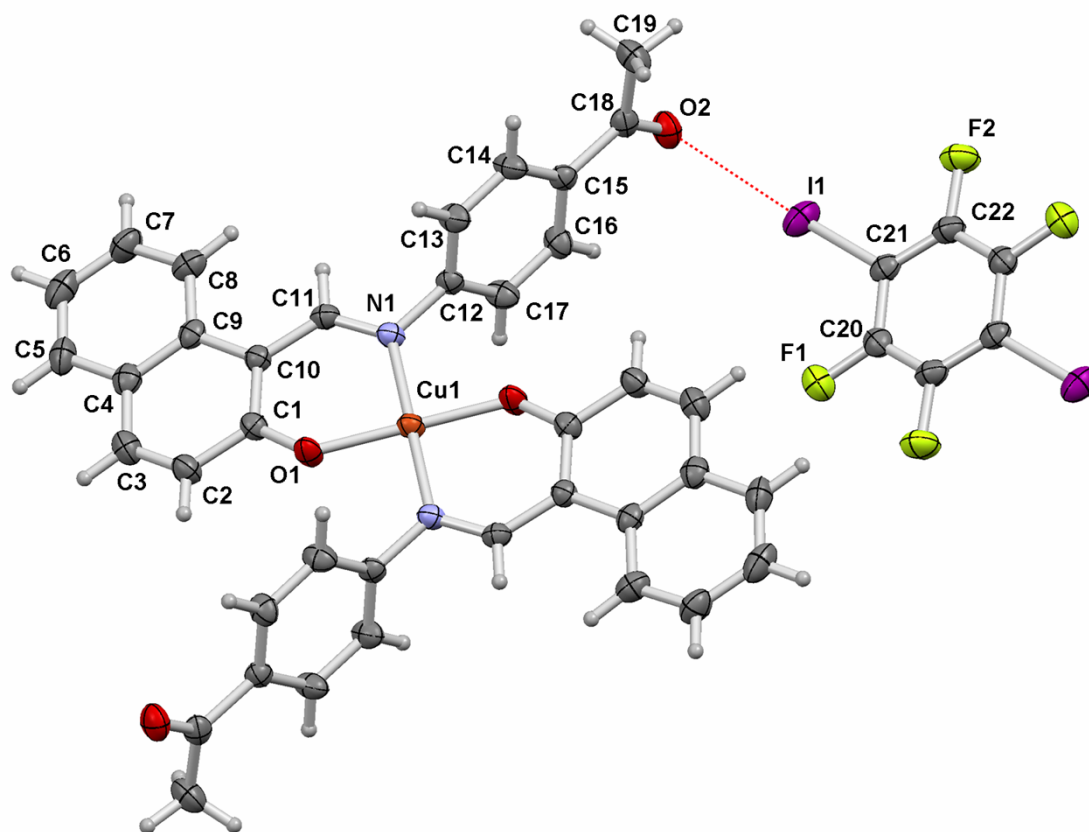


Figure S1. Molecular structures of Cu(naap)₂·tfib showing the atom-labelling scheme. Displacement ellipsoids are drawn at the 30 % probability level and H atoms are shown as small spheres of arbitrary radius.

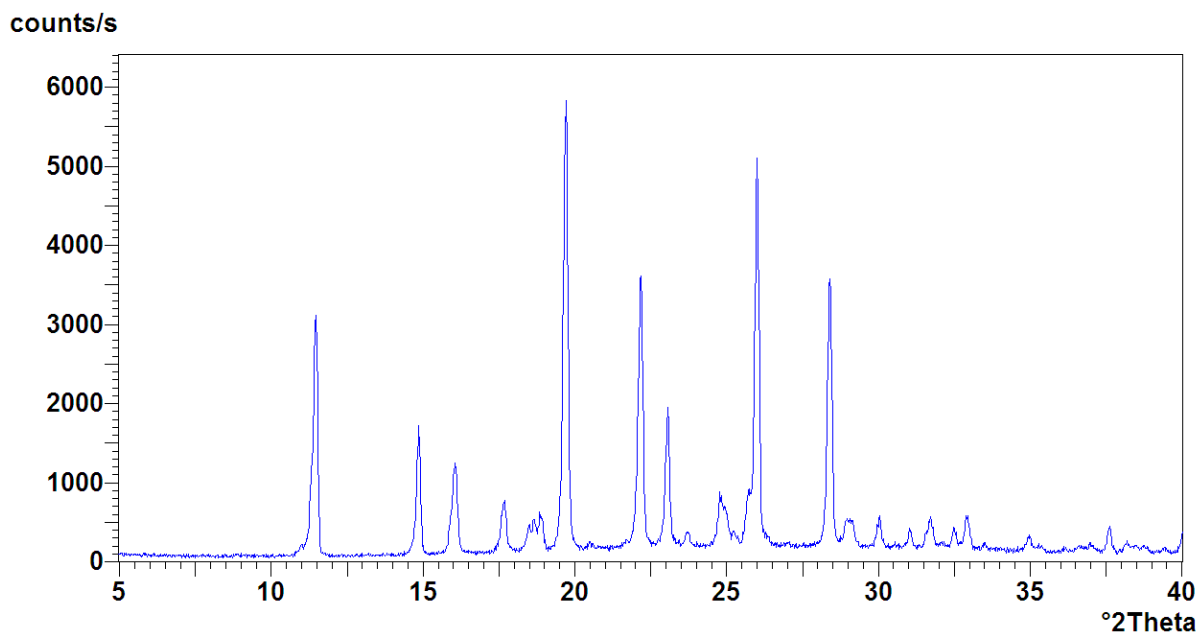


Figure S2. PXRD pattern of pure **napht** reactant.

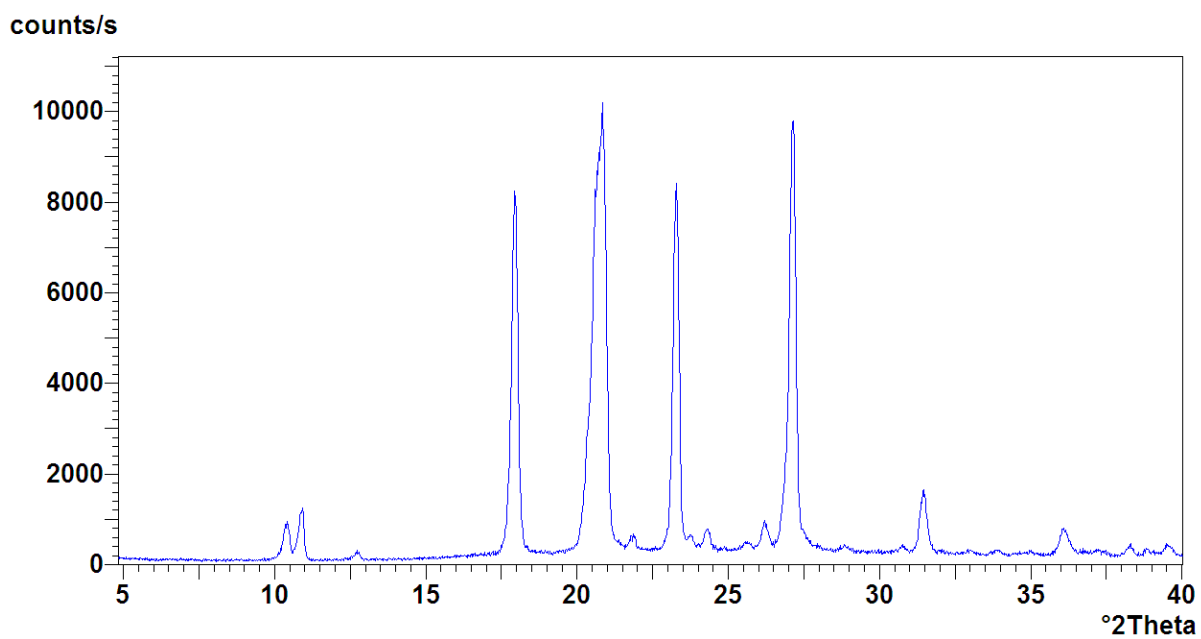


Figure S3. PXRD pattern of pure **aap** reactant.

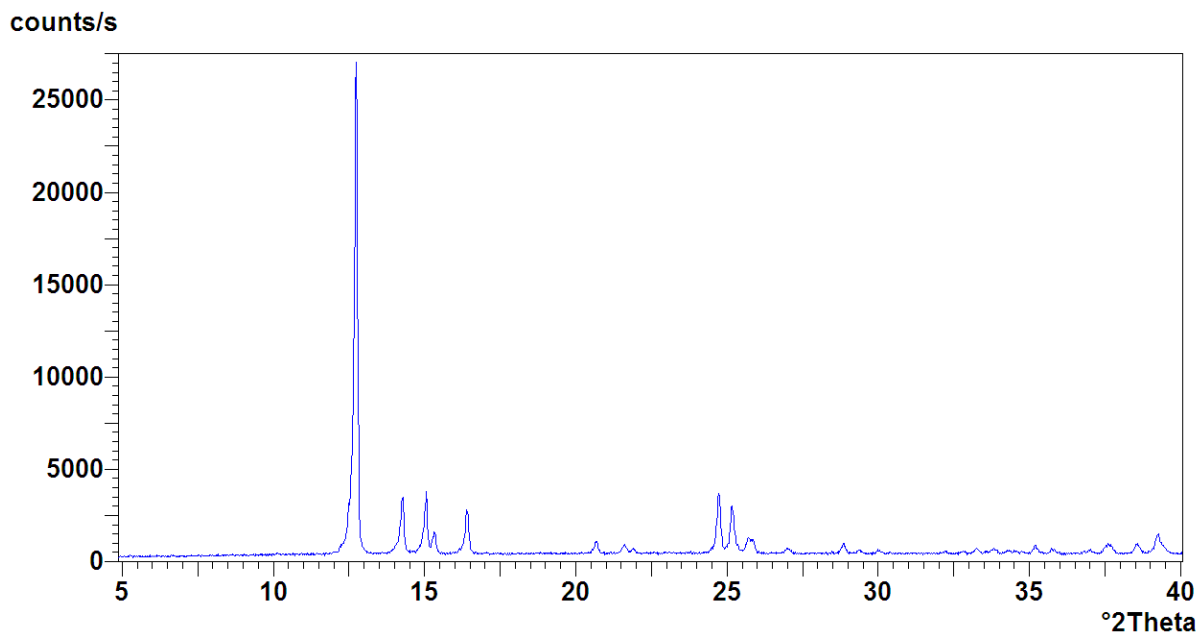


Figure S4. PXRD pattern of pure copper acetate monohydrate.

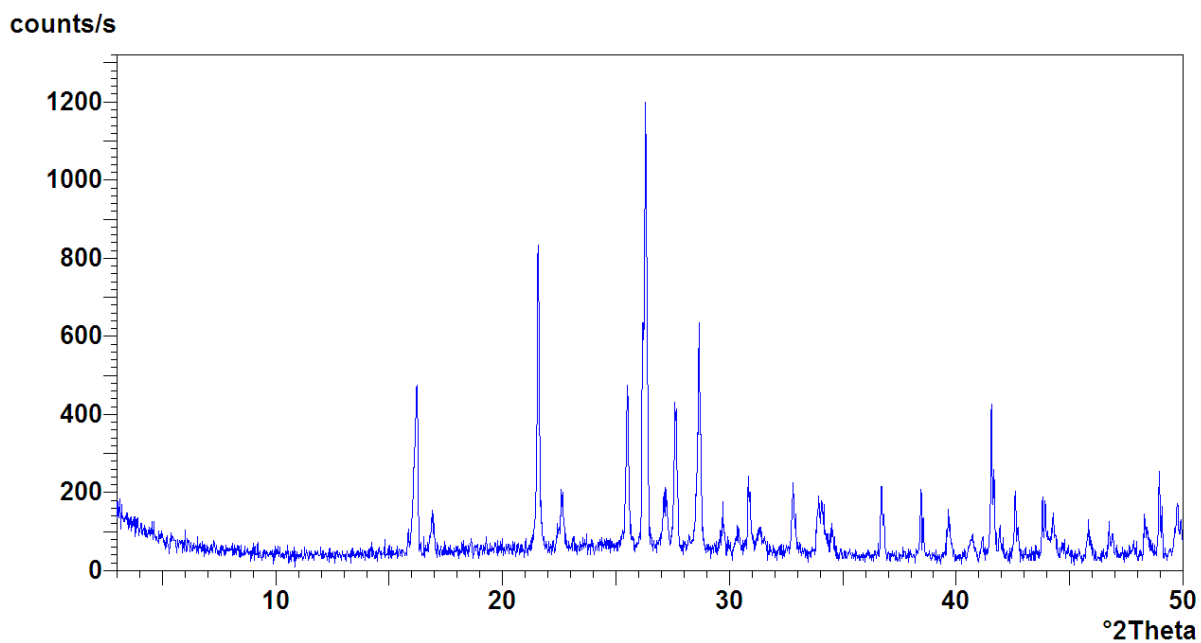


Figure S5. PXRD pattern of pure **tfib** reactant.

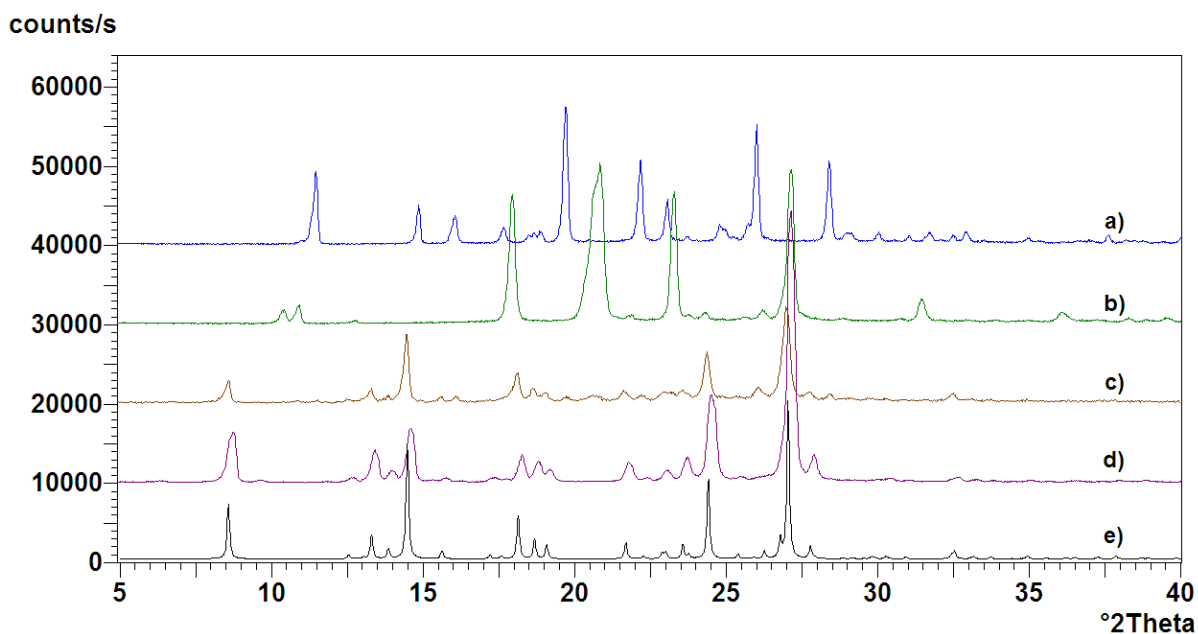


Figure S6. PXRD patterns for mechanochemical and solution-based experiments involving **naphth** and **aap**: a) **naphth**, b) **aap**, c) compound **Hnaap** obtained by grinding in ball mill for 60 min in the presence of a small quantity of a mixture of EtOH and TEA [5% v/v of TEA], d) compound **Hnaap** obtained by solution-based method, e) calculated pattern for compound **Hnaap**.

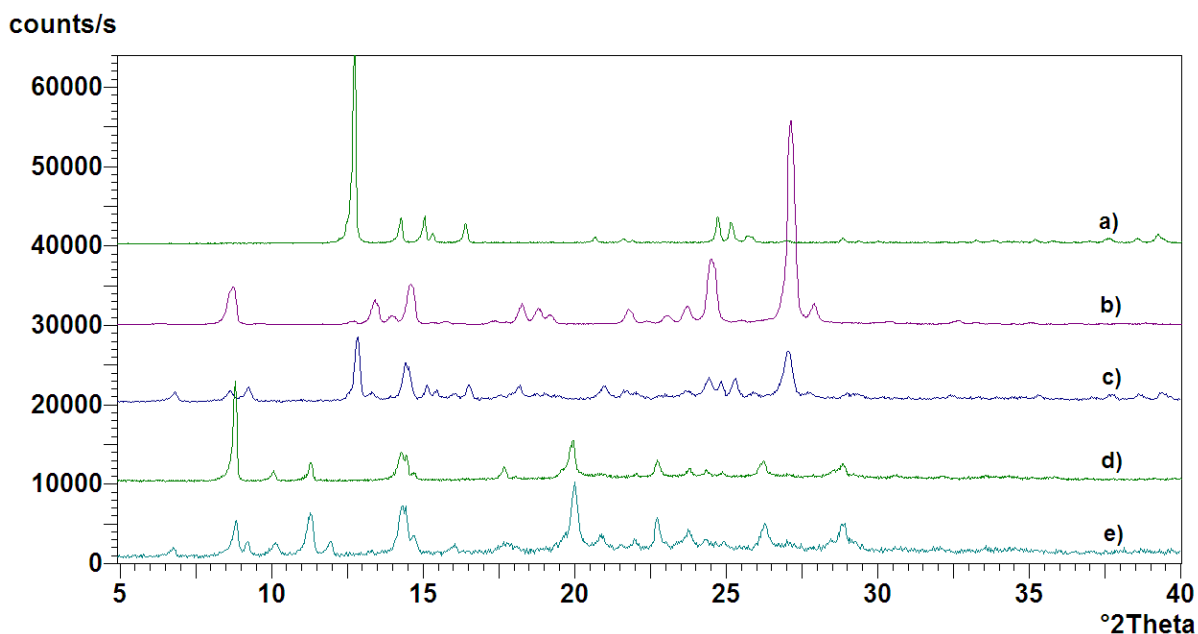


Figure S7. PXRD patterns for mechanochemical and solution-based experiments involving compound **Hnaap** and copper acetate monohydrate: a) compound **Hnaap**, b) copper acetate monohydrate, c) acetic acid solvate of $\text{Cu}(\text{naap})_2$ obtained by grinding in ball mill for 50 min in the presence of a small quantity of a mixture of EtOH and TEA [5% v/v of TEA], d) compound $\text{Cu}(\text{naap})_2$ obtained by solution-based method, e) acetic acid solvate of $\text{Cu}(\text{naap})_2$ after annealing at 200 °C for 30 min.

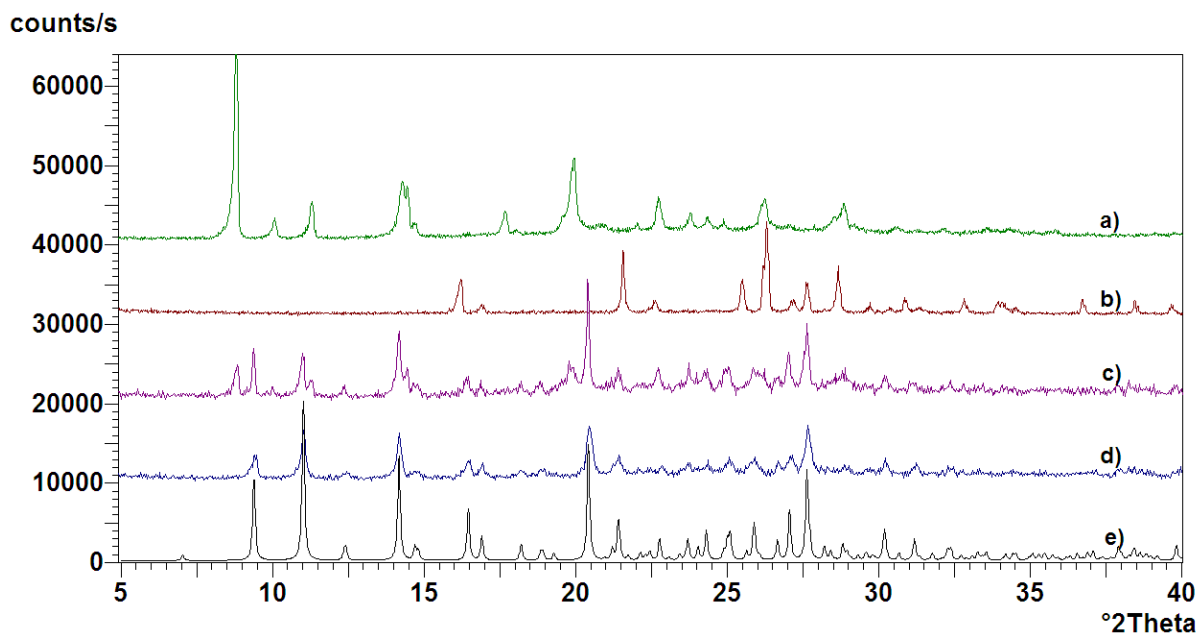


Figure S8. PXRD patterns for mechanochemical and solution-based experiments involving compound $\text{Cu}(\text{naap})_2$ and **tfib**: a) compound $\text{Cu}(\text{naap})_2$, b) **tfib**, c) compound $\text{Cu}(\text{naap})_2 \cdot \text{tfib}$ obtained by solution-based method, d) compound $\text{Cu}(\text{naap})_2 \cdot \text{tfib}$ obtained by grinding in ball mill for 50 min in the presence of a small quantity of nitromethane and e) calculated pattern for compound $\text{Cu}(\text{naap})_2 \cdot \text{tfib}$.

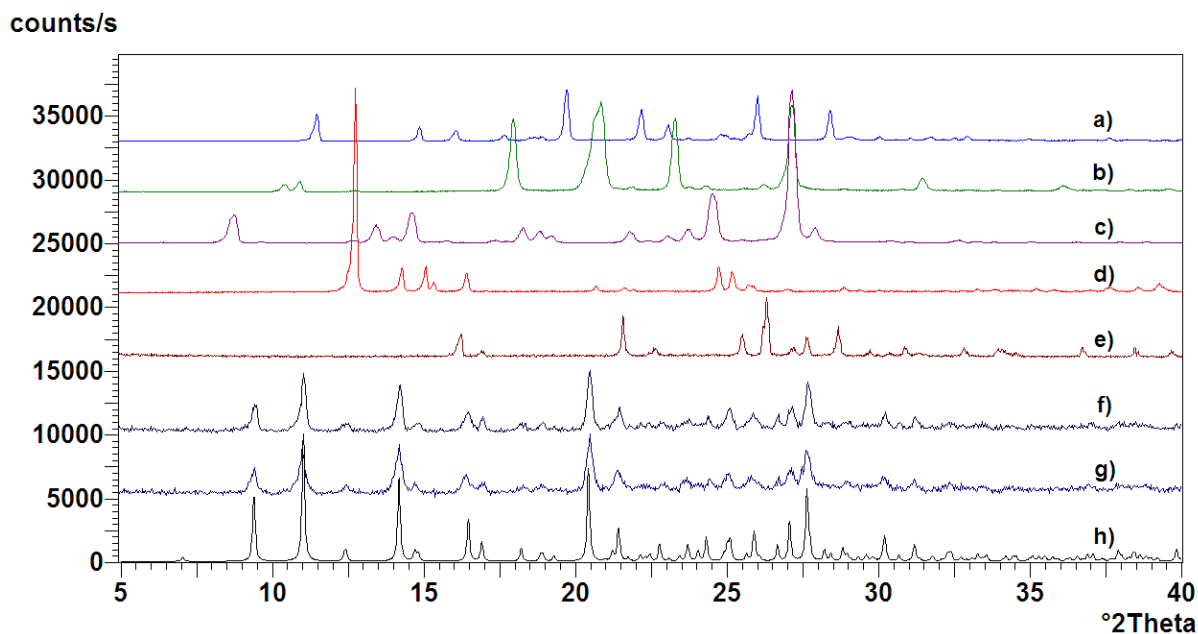


Figure S9. PXRD patterns for one-pot mechanochemical experiments: a) **napht**, b) **aap**, c) compound **Hnaap**, d) copper acetate monohydrate, e) **tfib**, f) compound $\text{Cu}(\text{naap})_2 \cdot \text{tfib}$ obtained by grinding of compound **Hnaap**, copper acetate monohydrate and **tfib** in ball mill for 50 min in the presence of a small quantity of nitromethane, g) compound $\text{Cu}(\text{naap})_2 \cdot \text{tfib}$ obtained by grinding of **napht**, **aap**, copper acetate monohydrate and **tfib** in ball mill for 60 min in the presence of a small quantity of nitromethane and h) calculated pattern for compound $\text{Cu}(\text{naap})_2 \cdot \text{tfib}$.

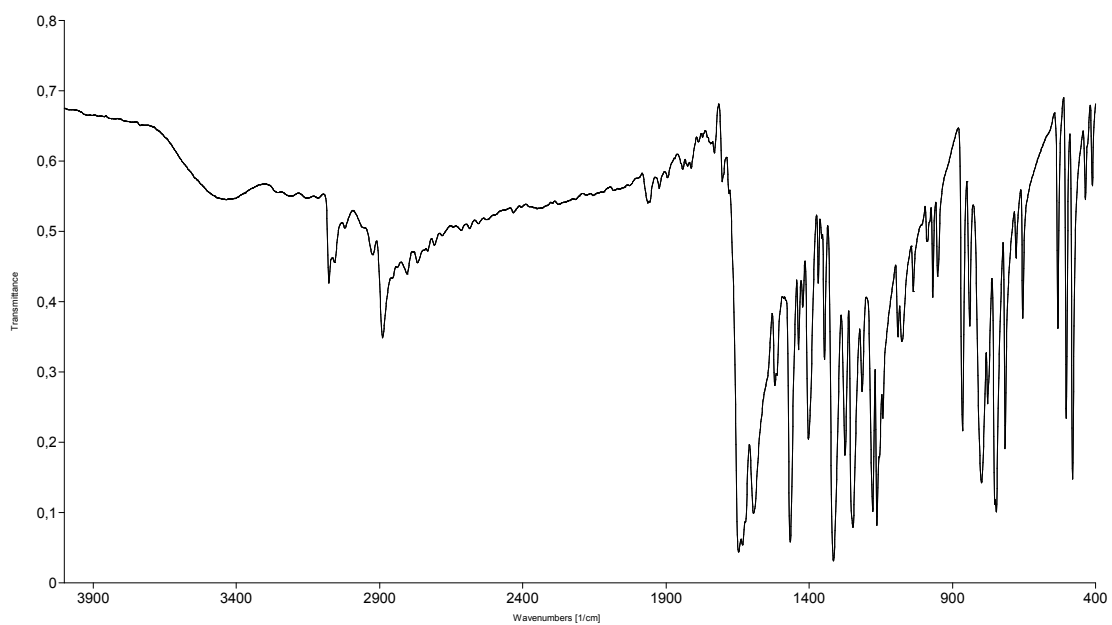


Figure S10. IR spectrum for pure **napht** reactant.

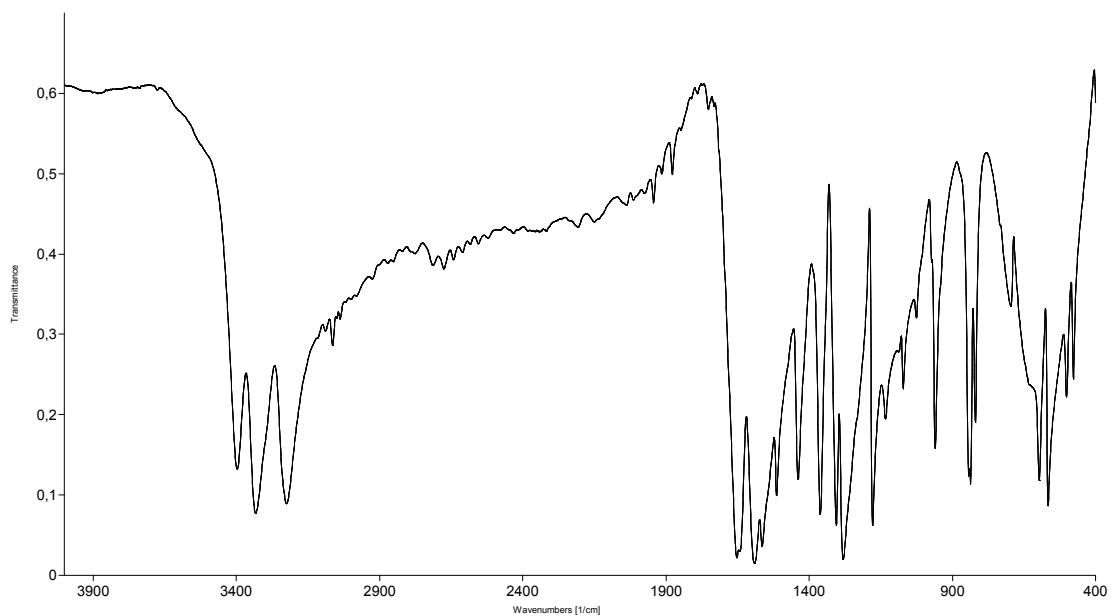


Figure S11. IR spectrum for pure **aap** reactant.

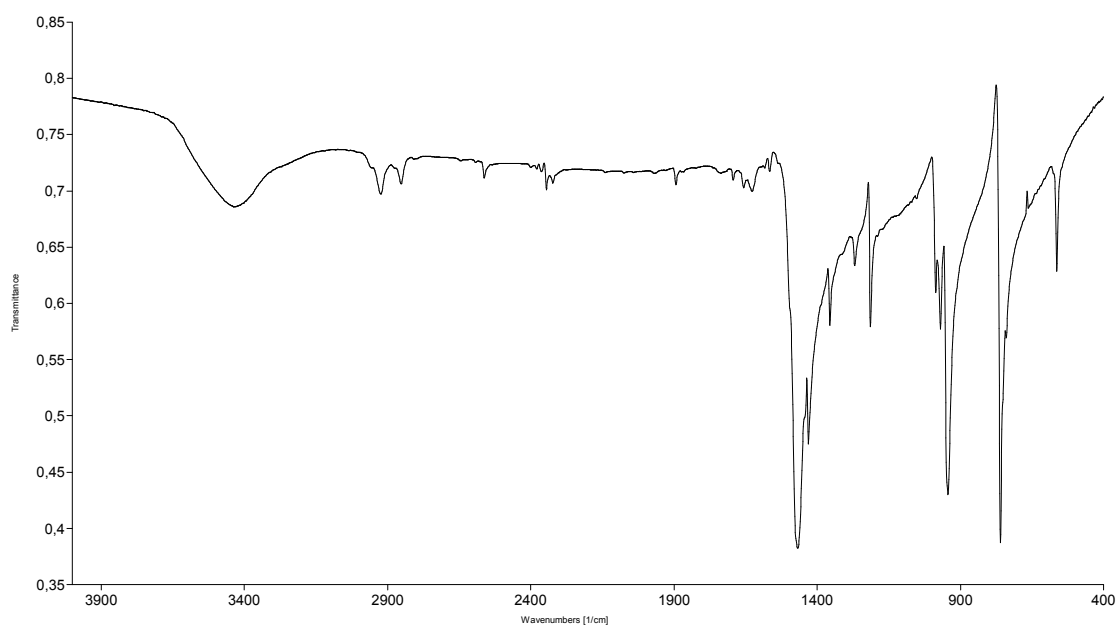


Figure S12. IR spectrum for pure **tfib** reactant.

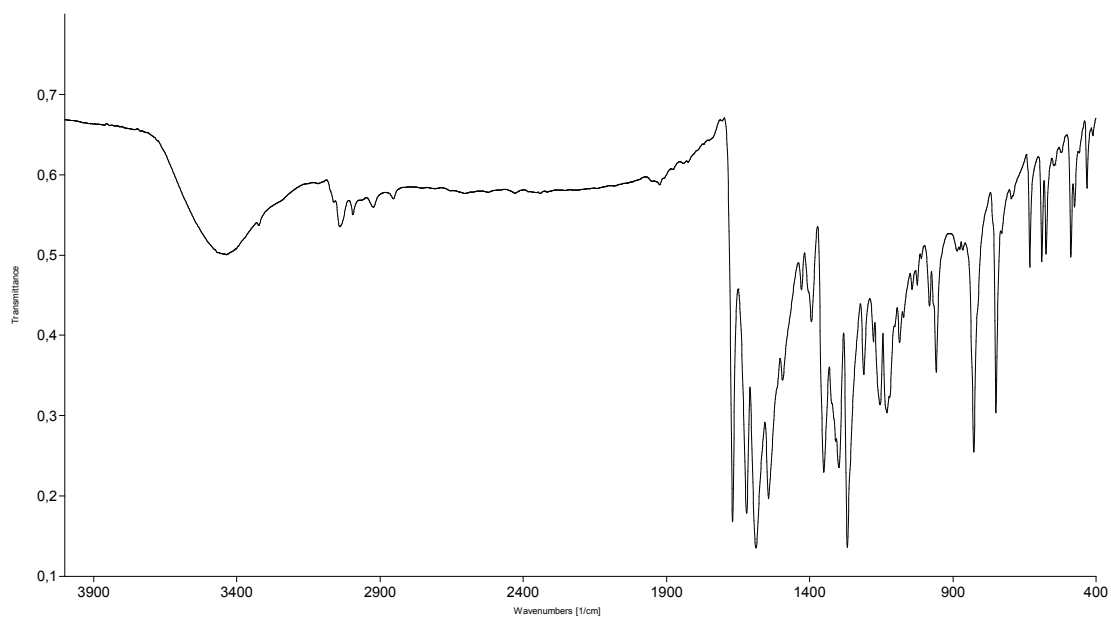


Figure S13. IR spectrum for **Hnaap** prepared by solution-based method.

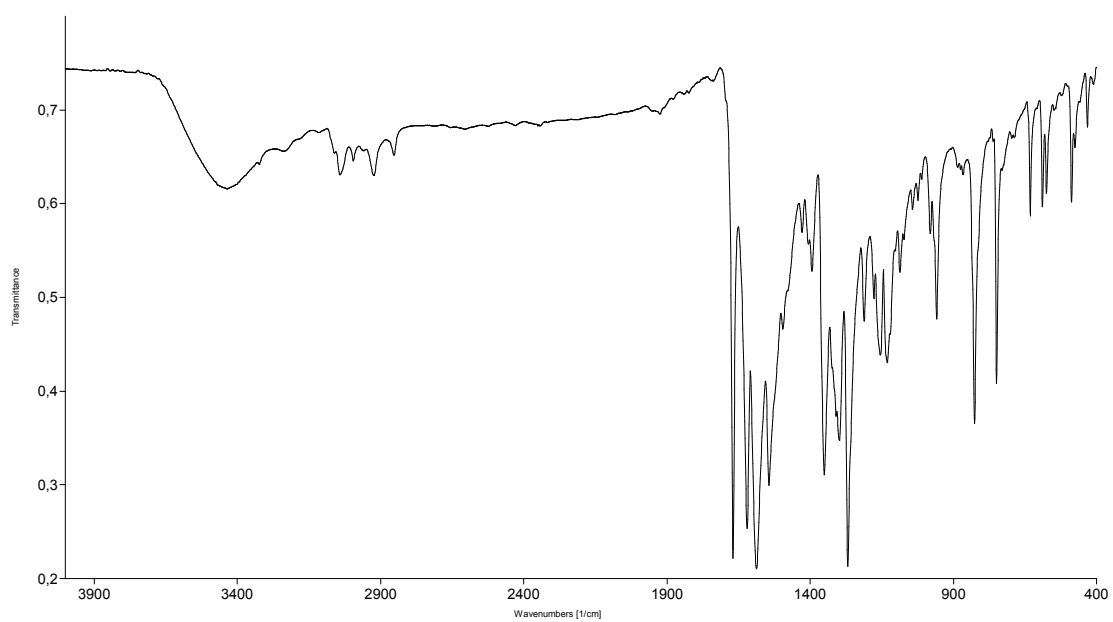


Figure S14. IR spectrum for **Hnaap** prepared by LAG.

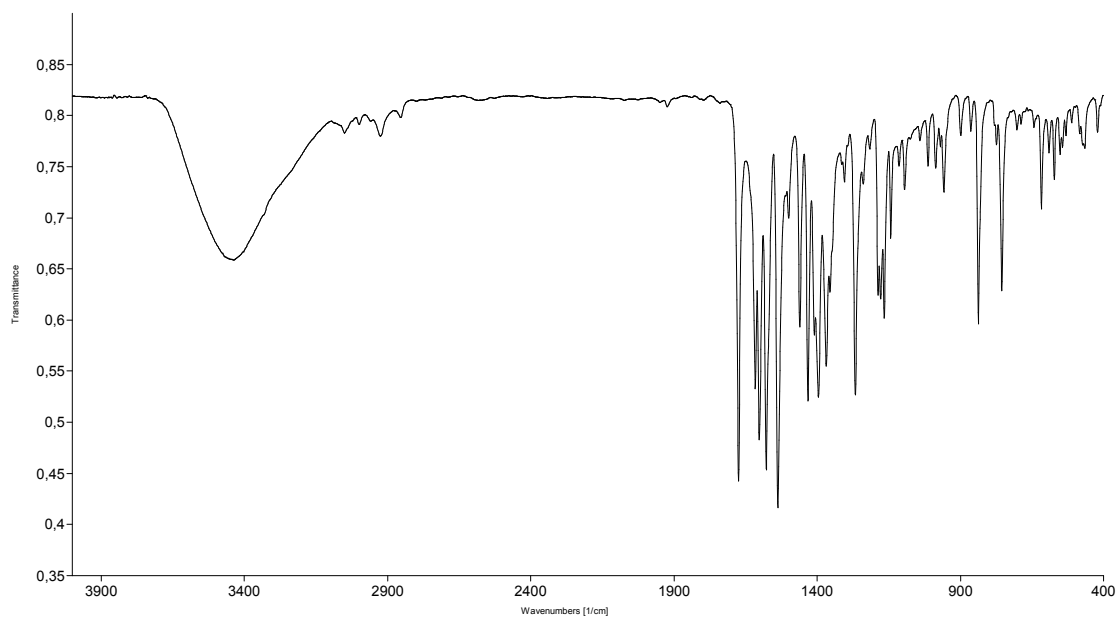


Figure S15. IR spectrum for **Cu(naap)₂** prepared by solution-based method.

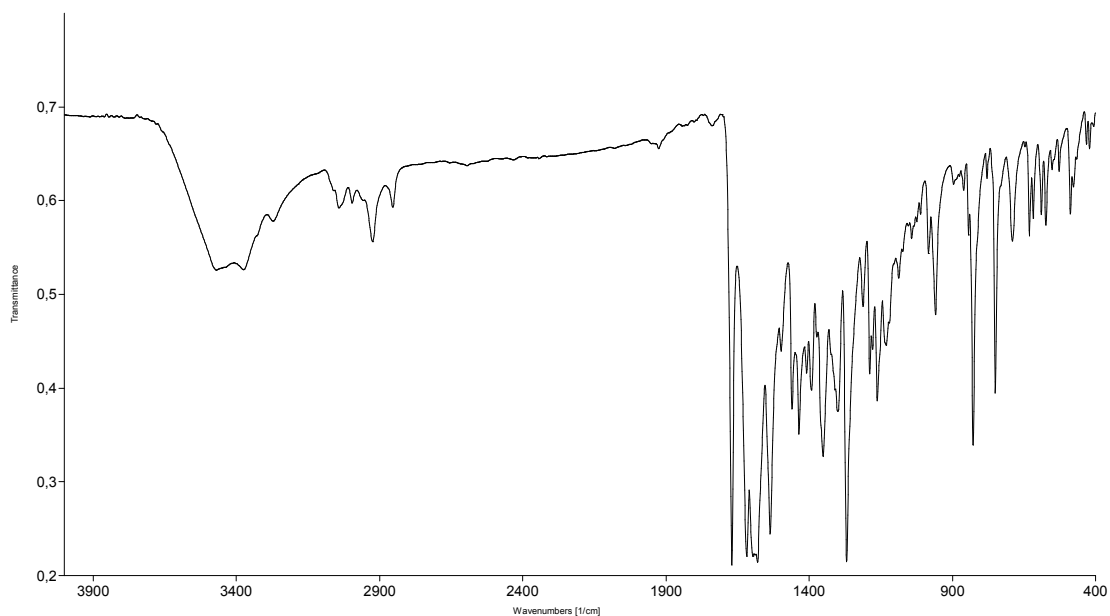


Figure S16. IR spectrum for the product of grinding of copper acetate monohydrate and compound **1**, i.e. the acetic acid solvate of compound $\text{Cu}(\text{naap})_2$.

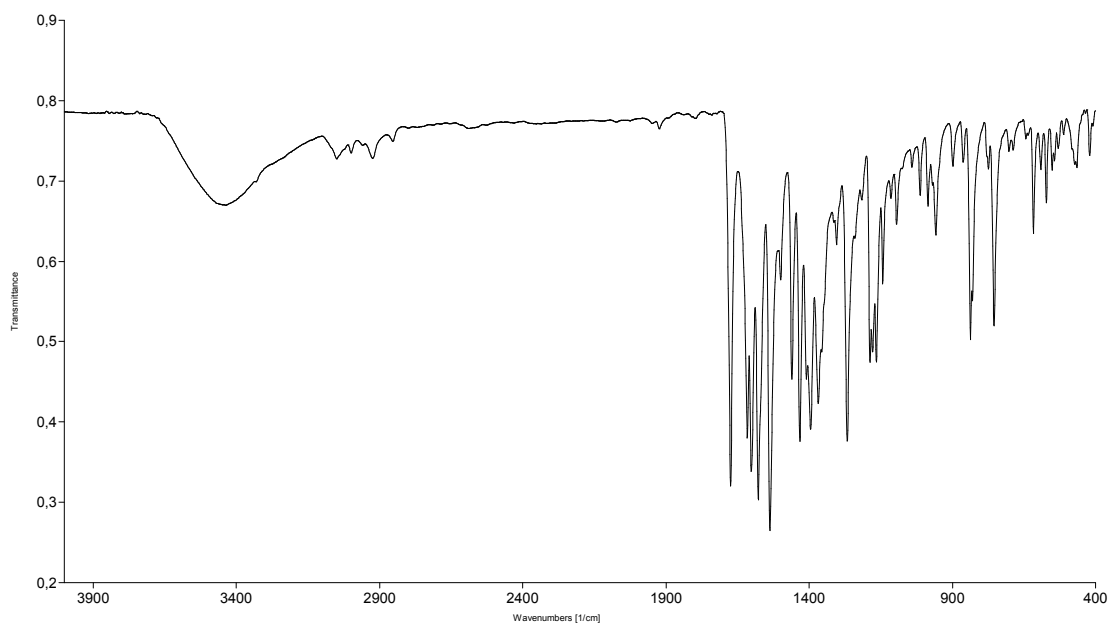


Figure S17. IR spectrum for the product of grinding of copper acetate monohydrate and compound **Hnaap** after isothermal experiment at 200 °C.

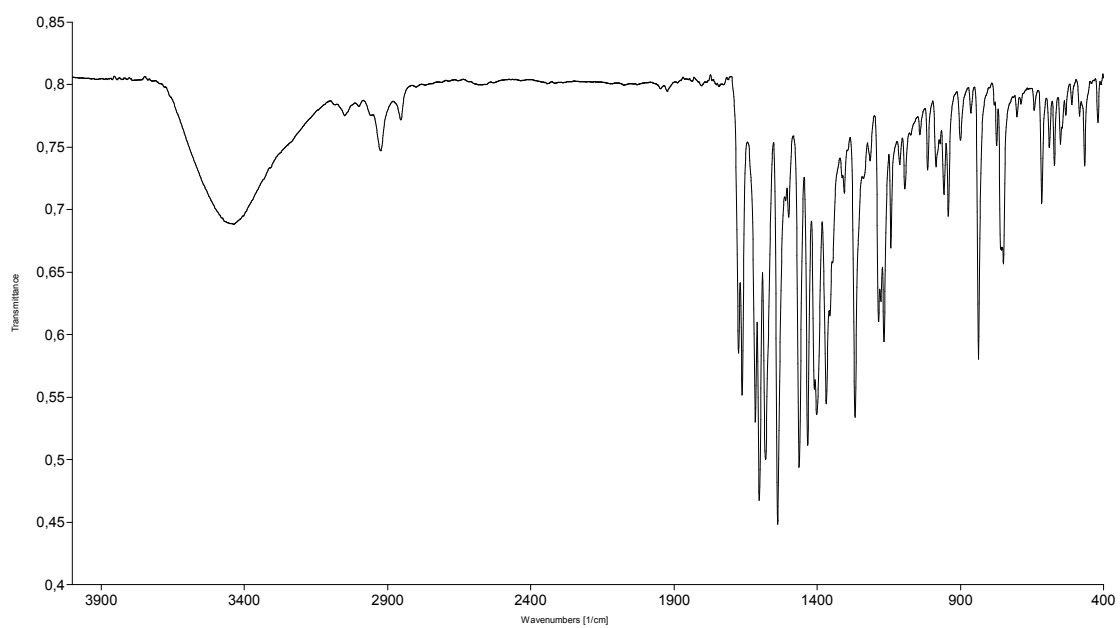


Figure S18. IR spectrum for $\text{Cu}(\text{naap})_2 \cdot \text{tfib}$ prepared by solution-based method.

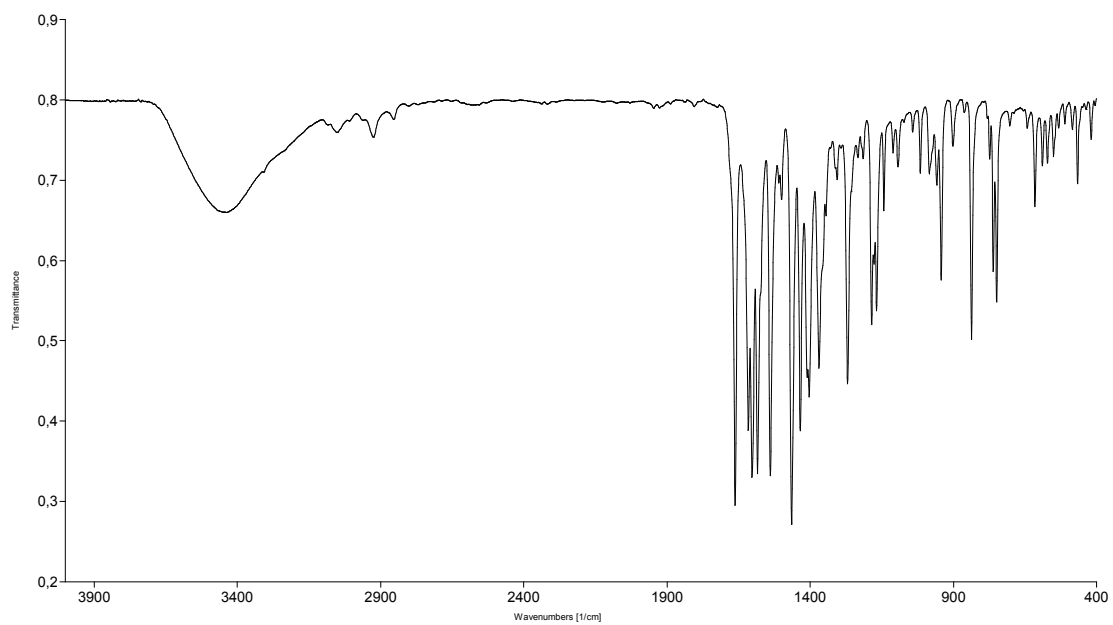


Figure S19. IR spectrum for $\text{Cu}(\text{naap})_2 \cdot \text{tfib}$ prepared by grinding of compound $\text{Cu}(\text{naap})_2$ and **tfib**.

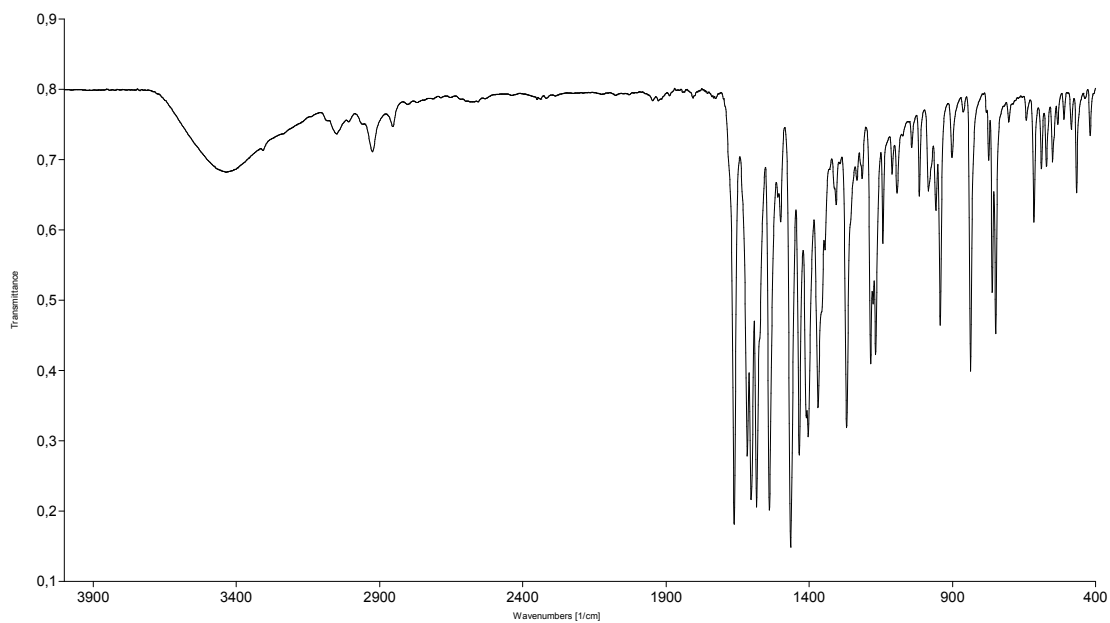


Figure S20. IR spectrum for $\text{Cu}(\text{naap})_2 \cdot \text{tfib}$ prepared by grinding of compound **Hnaap** and copper acetate monohydrate and **tfib**.

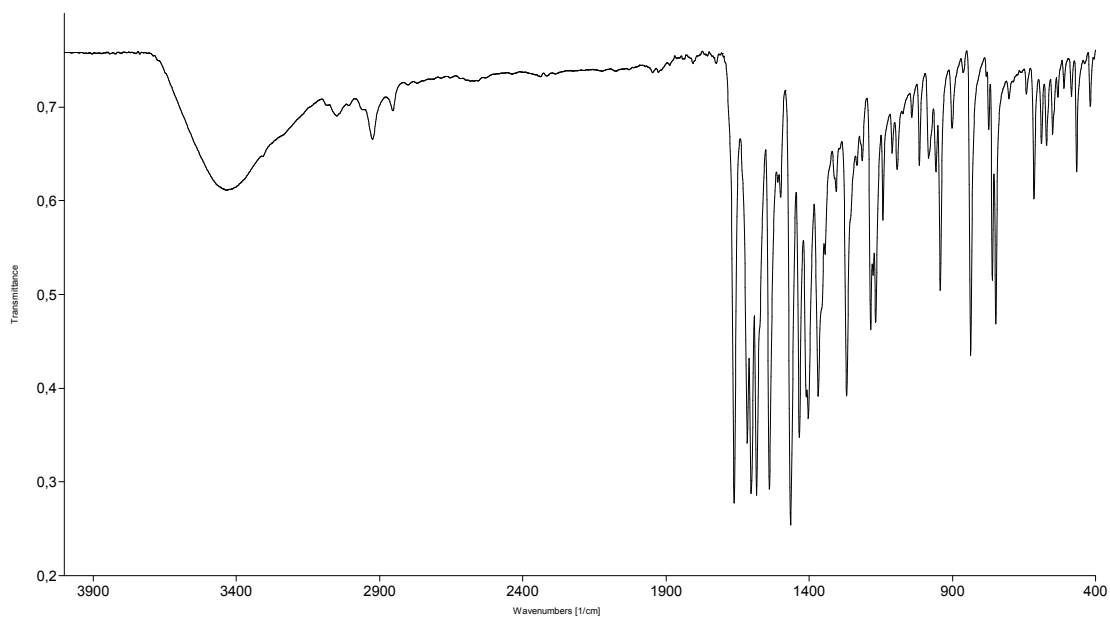


Figure S21. IR spectrum for $\text{Cu}(\text{naap})_2 \cdot \text{tfib}$ prepared by grinding of **napht**, **aap**, copper acetate monohydrate and **tfib**.

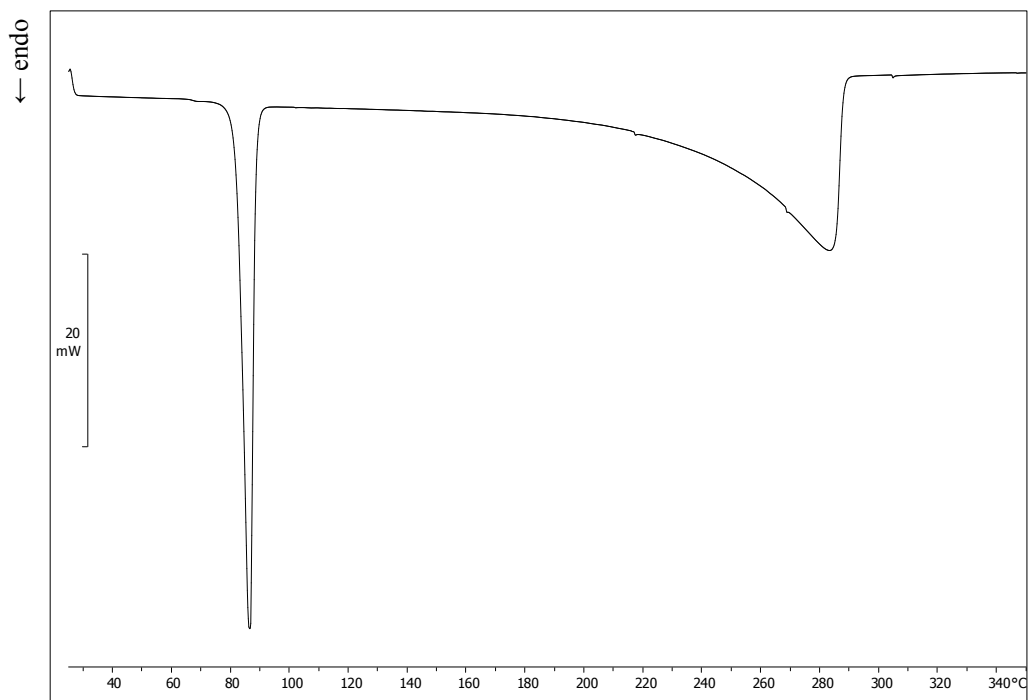


Figure S22. DSC curve for pure **naph** reactant.

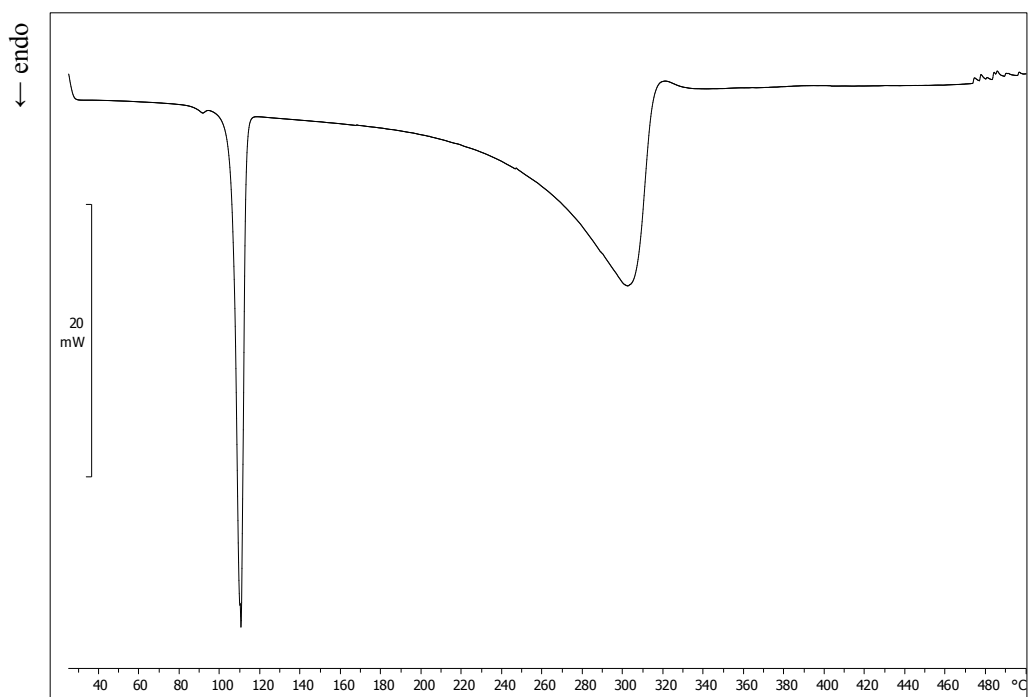


Figure S23. DSC curve for pure **aap** reactant.

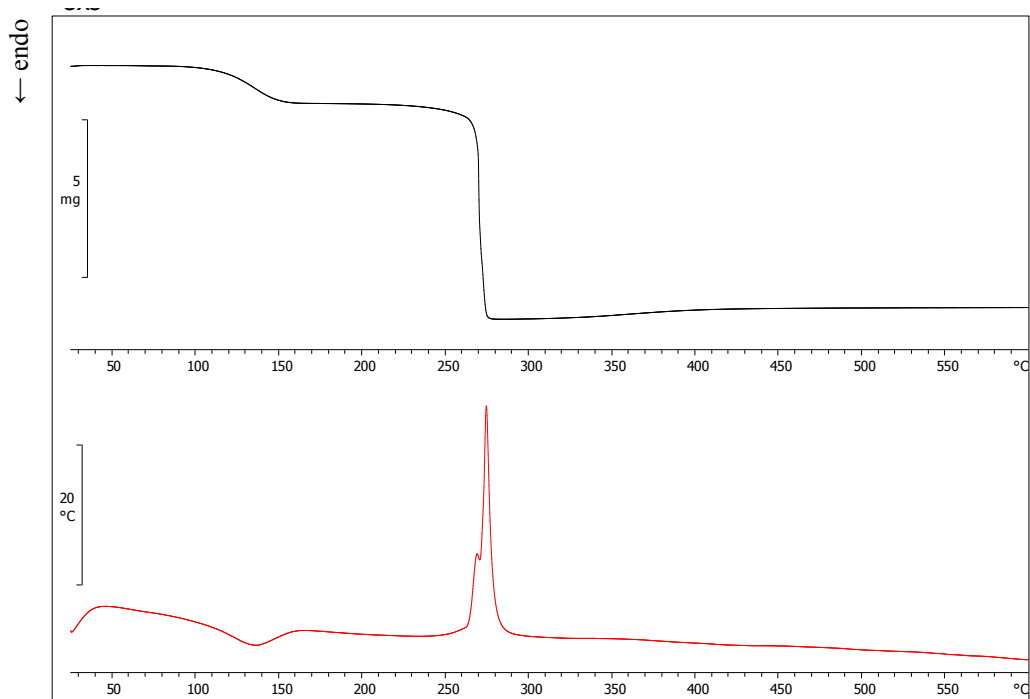


Figure S24. TG (black) and DTA (red) curve for pure copper acetate monohydrate.

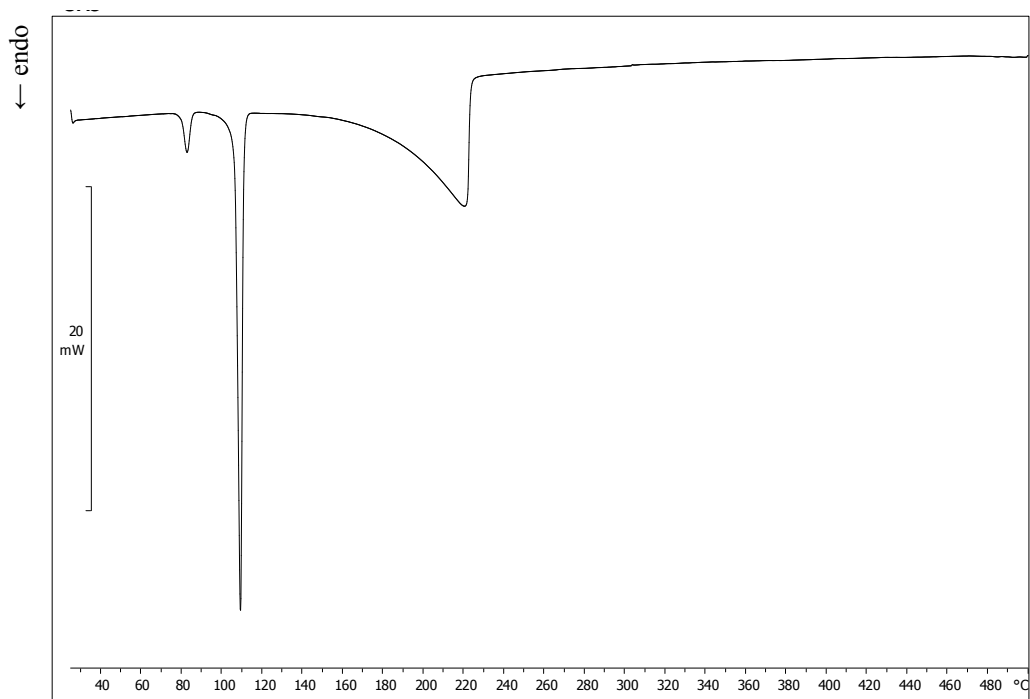


Figure S25. DSC curve for pure **tfib** reactant.

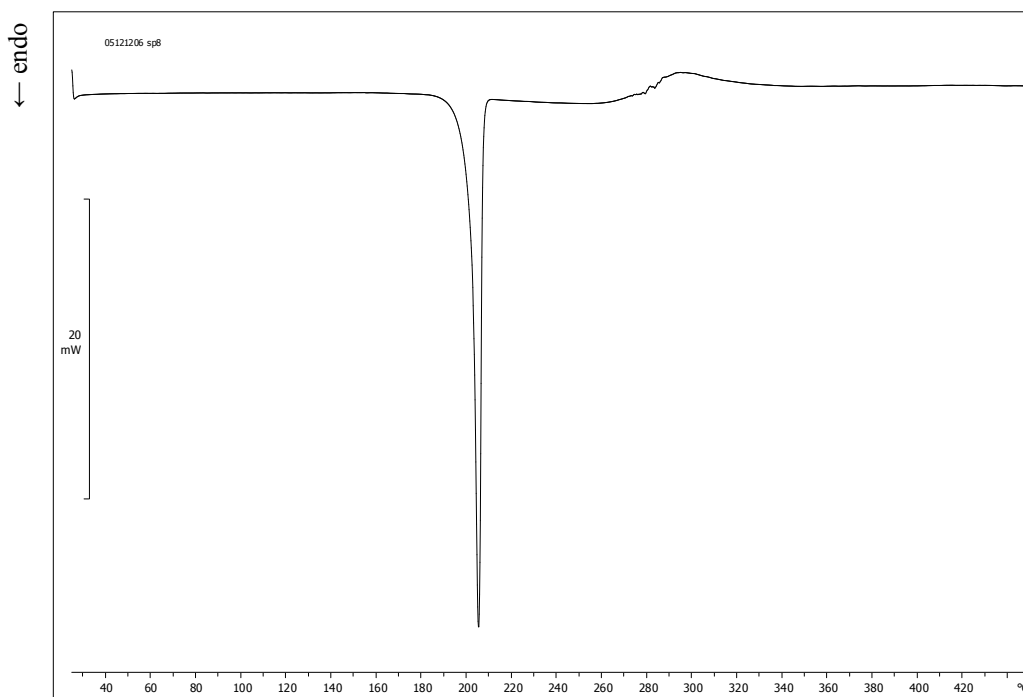


Figure S26. DSC curve for **Hnaap** synthesised by solution-based method.

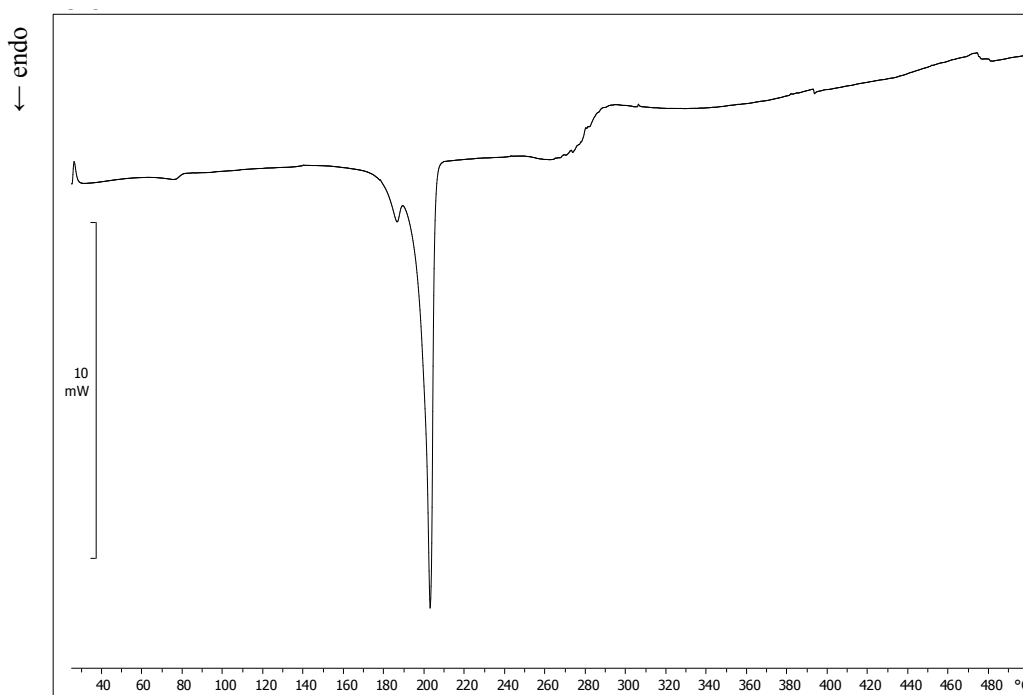


Figure S27. DSC curve for **Hnaap** synthesised by grinding in ball mill for 60 min in the presence of a small quantity of a mixture of EtOH and TEA [5% v/v of TEA].

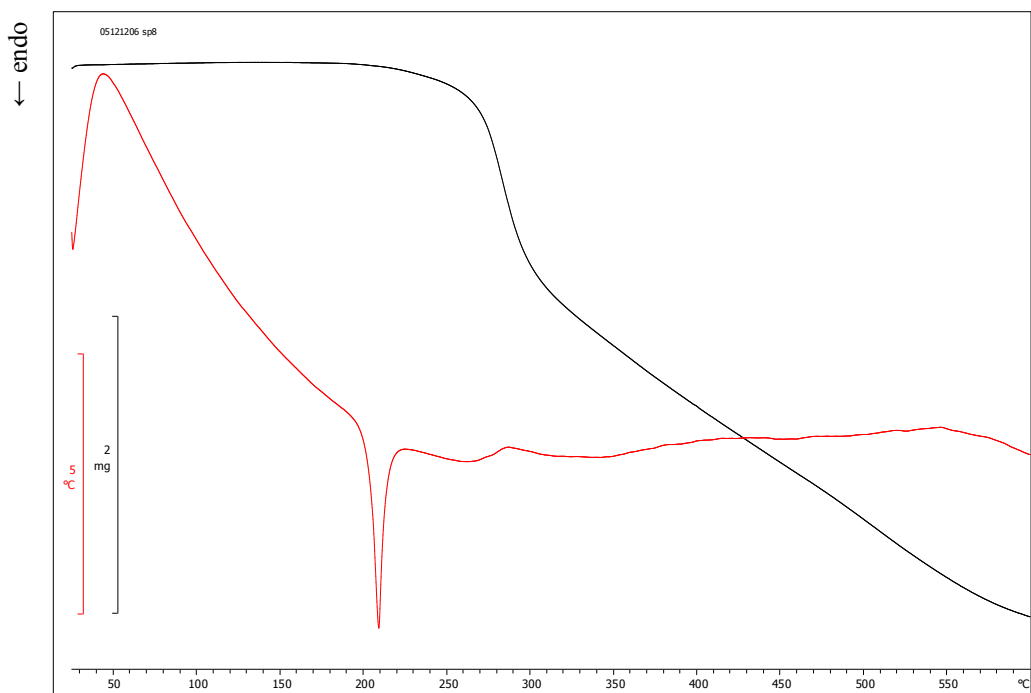


Figure S28. TG (black) and DTA (red) curve for **Hnaap** synthesised by solution-based method.

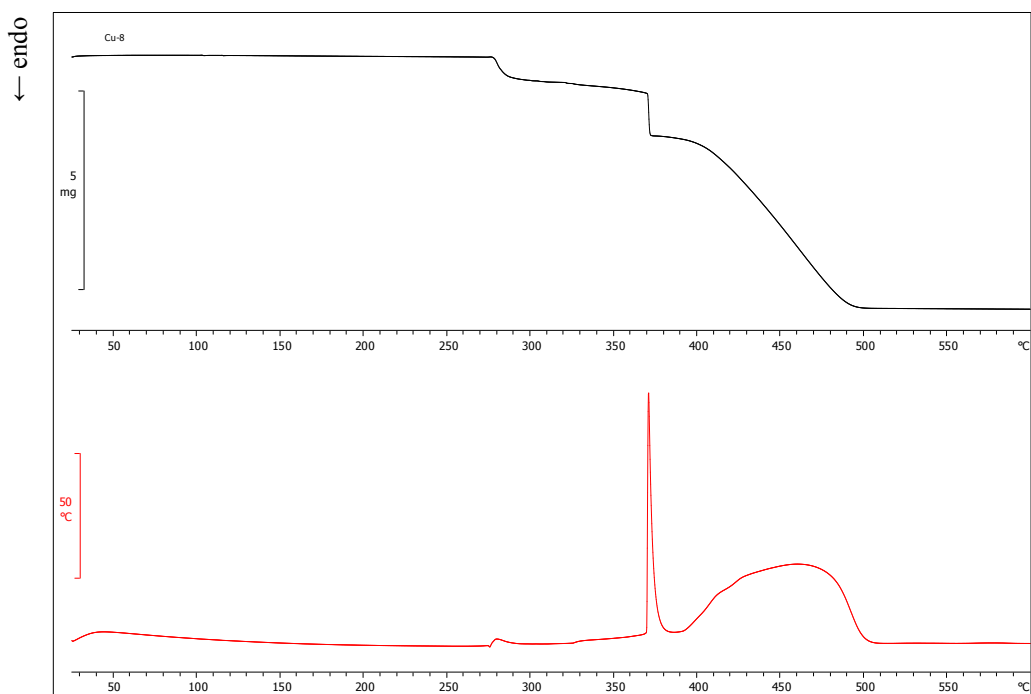


Figure S29. TG (black) and DTA (red) curve for **Cu(naap)₂** obtained by solution-based method.

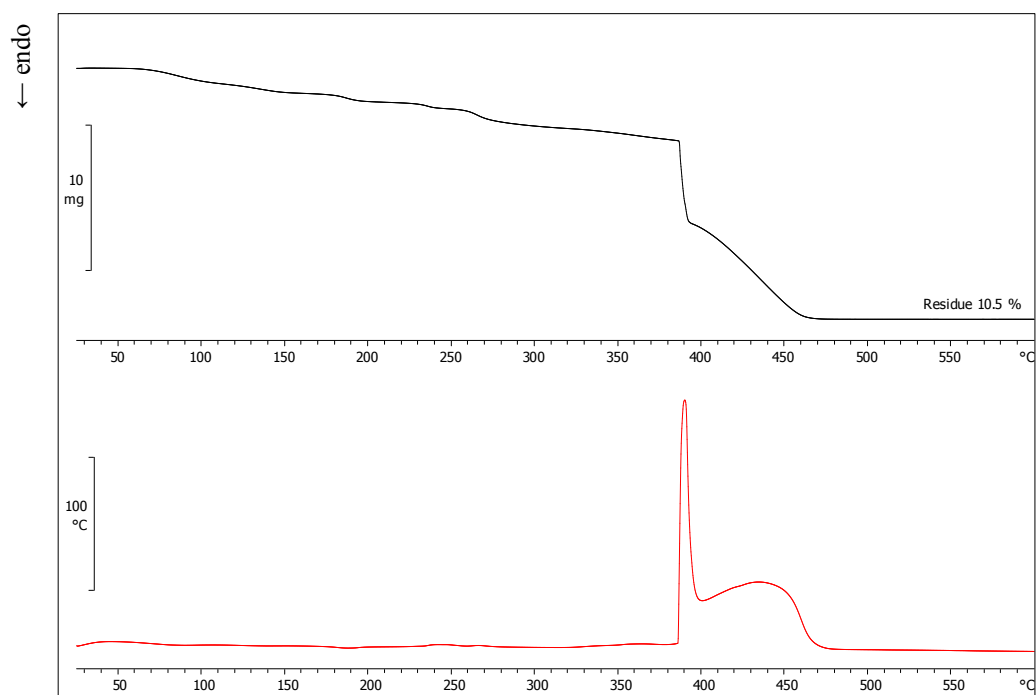


Figure S30. TG (black) and DTA (red) curve for the product (i.e. the acetic acid solvate of compound $\text{Cu}(\text{naap})_2$) obtained by grinding of copper acetate and compound **Hnaap** in ball mill for 60 min in the presence of a small quantity of a mixture of EtOH and TEA [5% v/v of TEA].

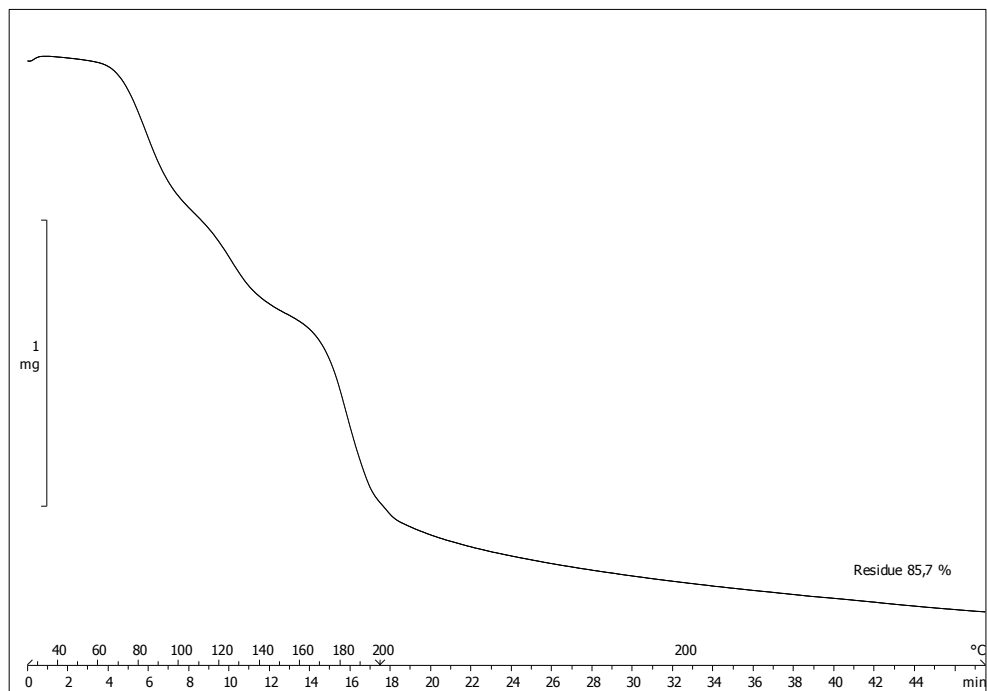


Figure S31. TG curve of isothermal experiment at 200 °C for the product of grinding of copper acetate monohydrate and compound **Hnaap**, i.e. the acetic acid solvate of compound $\text{Cu}(\text{naap})_2$.

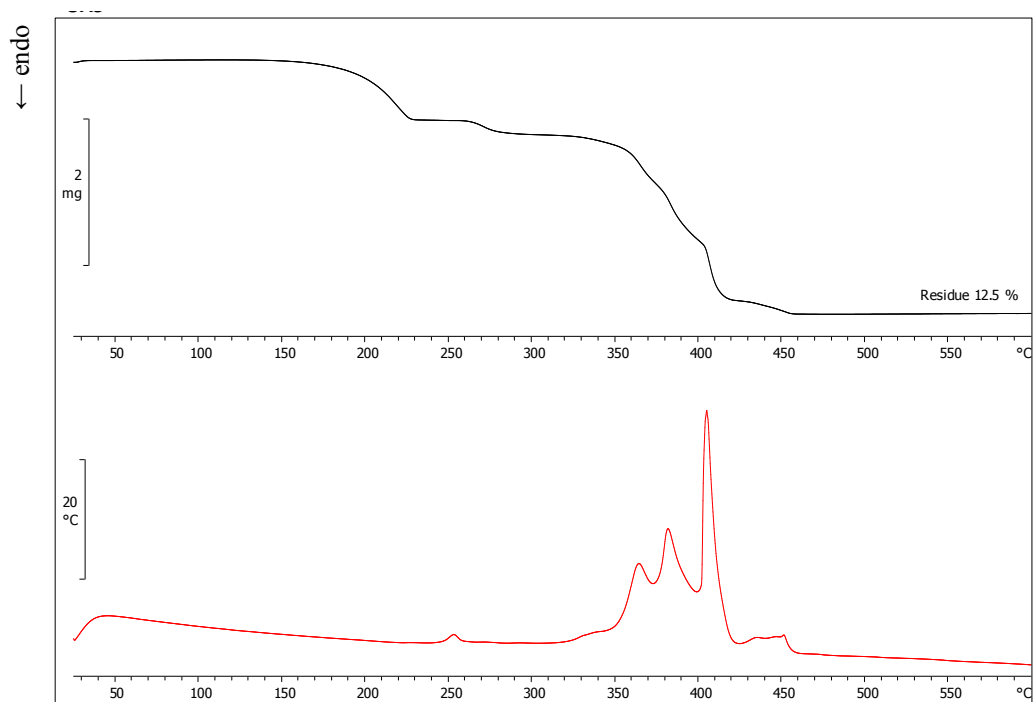


Figure S32. TG (black) and DTA (red) curve for $\text{Cu}(\text{naap})_2 \cdot \text{tfib}$ obtained by solution-based method.

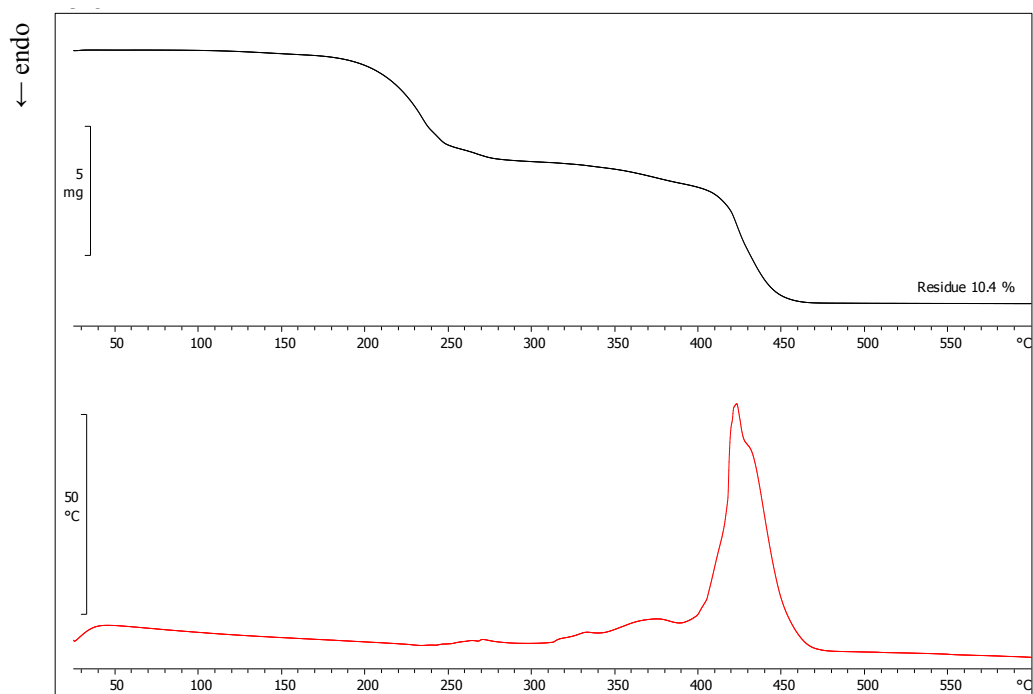


Figure S33. TG (black) and DTA (red) curve for $\text{Cu}(\text{naap})_2 \cdot \text{tfib}$ obtained by grinding of compound $\text{Cu}(\text{naap})_2$ and **tfib** in ball mill for 60 min in the presence of a small quantity of nitromethane.

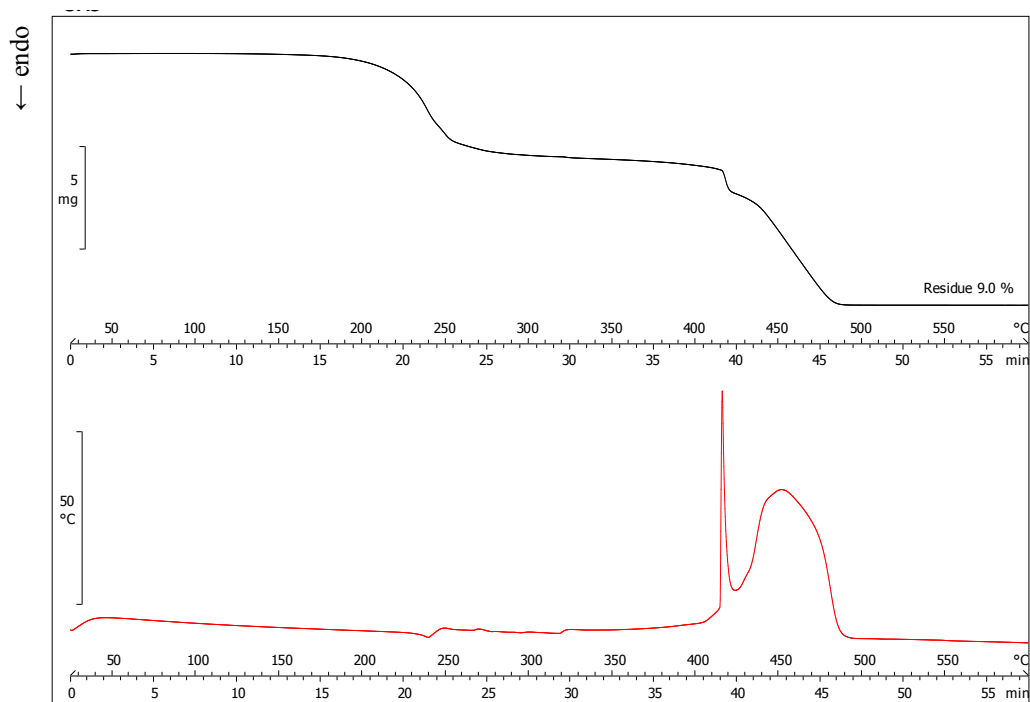


Figure S34. TG (black) and DTA (red) curve for $\text{Cu}(\text{naap})_2 \cdot \text{tfib}$ obtained by grinding of copper acetate monohydrate, compound **Hnaap** and **tfib** in ball mill for 60 min in the presence of a small quantity of a mixture of EtOH and TEA [5% v/v of TEA].

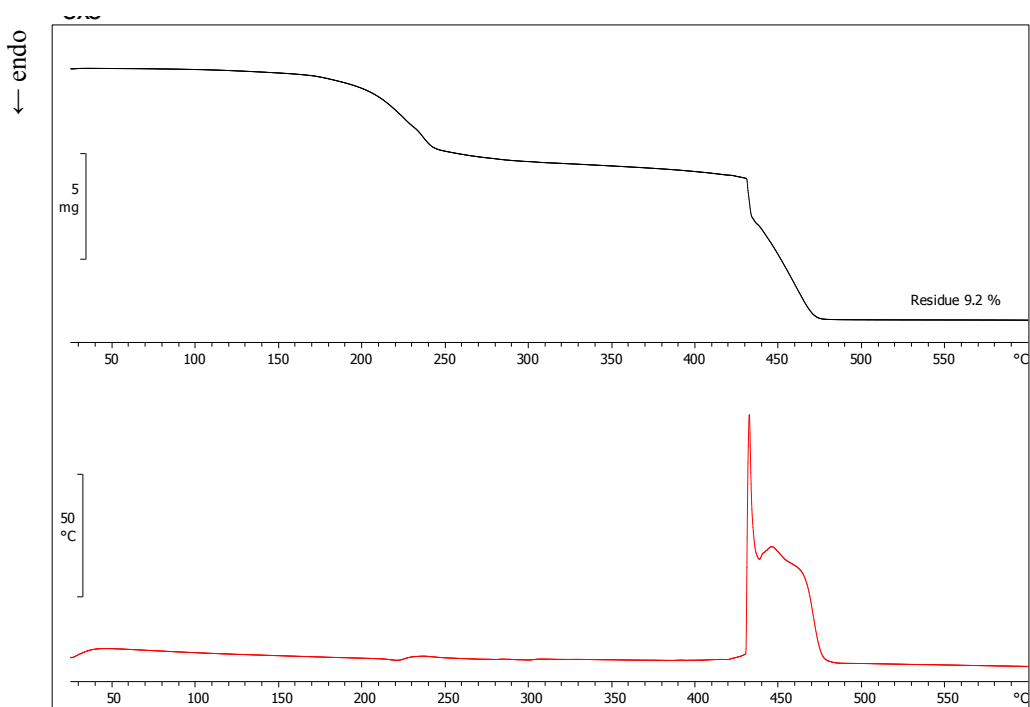


Figure S35. TG (black) and DTA (red) curve for $\text{Cu}(\text{naap})_2 \cdot \text{tfib}$ obtained by grinding of copper acetate monohydrate, **napht**, **aap** and **tfib** in ball mill for 60 min in the presence of a small quantity of a mixture of EtOH and TEA [5% v/v of TEA].

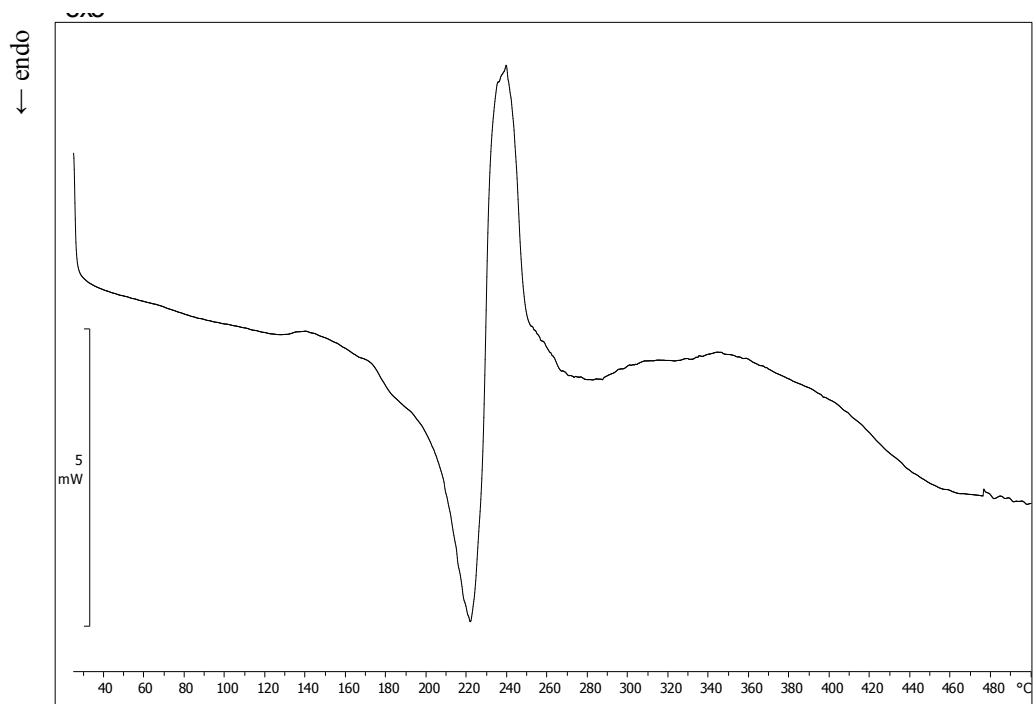


Figure S36. DSC curve for Cu(naap)₂·tfib obtained by grinding of copper acetate monohydrate, **napht**, **aap** and **tfib** in ball mill for 60 min in the presence of a small quantity of a mixture of EtOH and TEA [5% v/v of TEA].

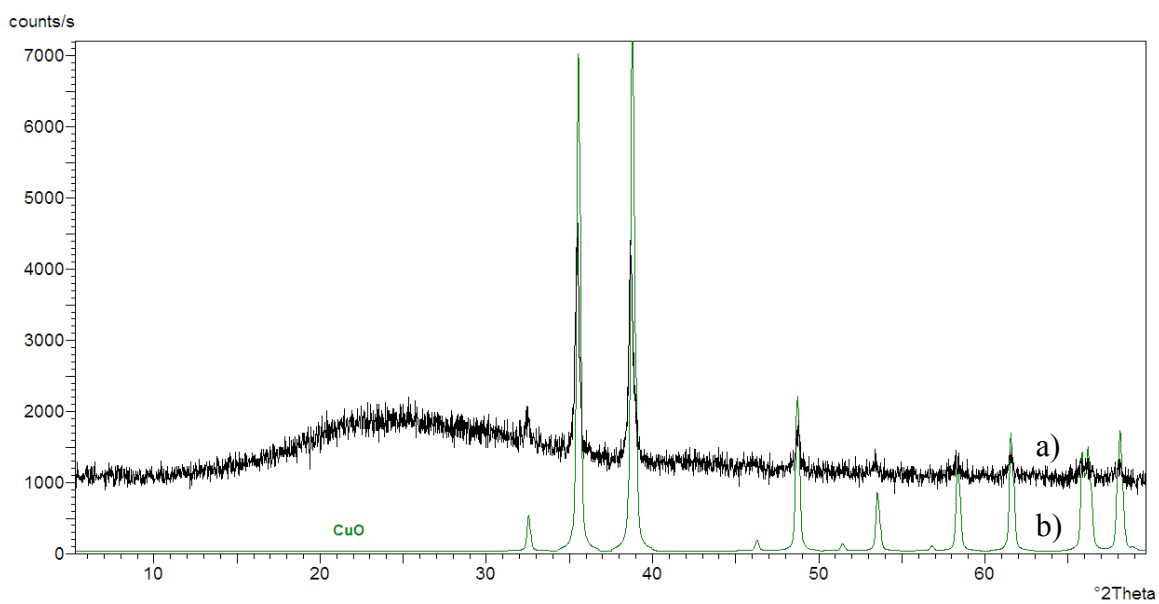


Figure S37. a) PXRD pattern of residue after TG experiment of compound $\text{Cu}(\text{naap})_2$ and b) calculated pattern for CuO .

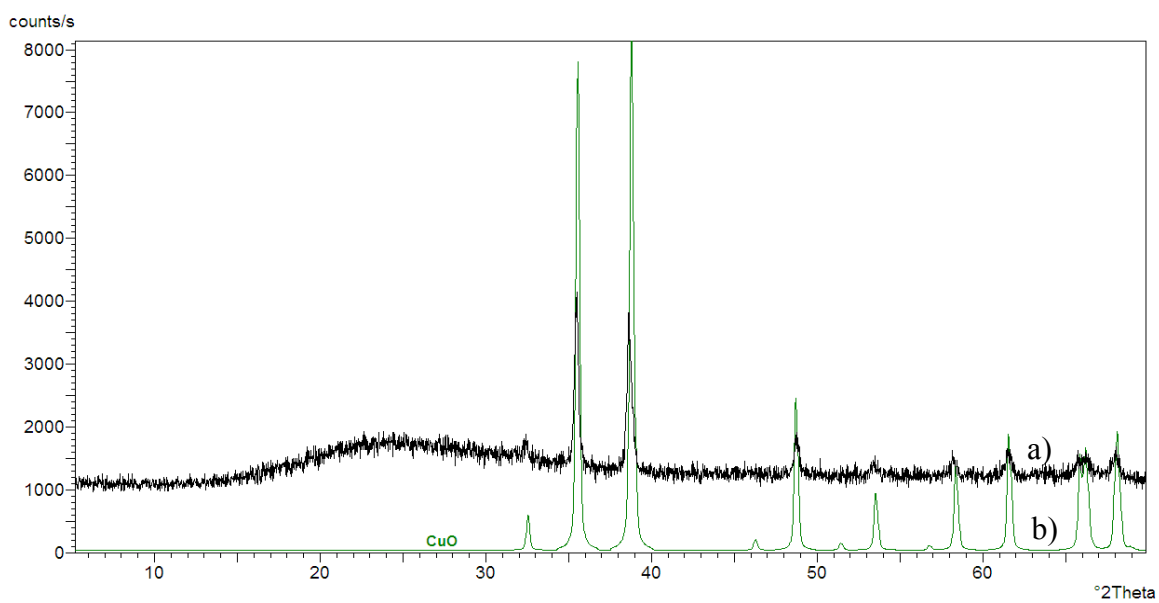


Figure S38. a) PXRD pattern of residue after TG experiment of compound $\text{Cu}(\text{naap})_2 \cdot \text{tfib}$ and b) calculated pattern for CuO .